



Article

A Truthful Mechanism for Multibase Station Resource Allocation in Metaverse Digital Twin Framework

Jixian Zhang ^{1,*} , Mingyi Zong ¹ and Weidong Li ² ¹ School of Information Science and Engineering, Yunnan University, Kunming 650504, China² School of Mathematics and Statistics, Yunnan University, Kunming 650504, China

* Correspondence: zhangjixian@ynu.edu.cn

Abstract: The concept of the metaverse has gained increasing attention in recent years, and the development of various new technologies, including digital twin technology, has made it possible to see the metaverse coming to pass. Many academics have begun to investigate various problems after realizing the importance of digital twin technology in building the metaverse. However, when utilizing digital twin technology to construct a metaverse, there remains limited research on how to allocate multibase station resources. This research translates a multibase station wireless resource allocation problem into an integer linear programming constraint model when virtual service providers construct a metaverse. In addition, the optimal VCG reverse auction (OPT-VCGRA) mechanism is designed to maximize social welfare and solve the problem of IoT devices competing for base station wireless resources. Specifically, the problem of the optimal allocation of wireless channel resources and payment rule based on the Vickrey–Clarke–Groves mechanism is solved to achieve optimal allocation and calculation of payment prices. Since the optimal allocation problem is NP-hard, this paper also designs a metaverse digital twin resource allocation and pricing (MDTRAP) mechanism based on monotonic allocation and key value theory. The mechanism sends the resource allocation results of multiple base stations to IoT devices and calculates the price payment when building a metaverse in the real world. This paper shows that both auction mechanisms have incentive compatibility and individual rationality properties. Through experiments, this paper compares the two mechanisms in terms of social welfare, the number of winners, and the overall payment. The MDTRAP mechanism performs similarly to the OPT-VCGRA mechanism in terms of social welfare, the number of winners, and channel utilization but is far superior to the OPT-VCGRA mechanism in terms of execution time and total payment. The truthful experiment also verified the truthfulness of the MDTRAP mechanism. The experimental results show that the MDTRAP mechanism can be used to solve the resource allocation problem of multiple base stations to IoT devices when building a metaverse in the real world and can effectively maximize social welfare.



Citation: Zhang, J.; Zong, M.; Li, W. A Truthful Mechanism for Multibase Station Resource Allocation in Metaverse Digital Twin Framework. *Processes* **2022**, *10*, 2601. <https://doi.org/10.3390/pr10122601>

Academic Editors: Danyu Bai, Xin Chen, Dehua Xu and Jędrzej Musiał

Received: 20 October 2022

Accepted: 1 December 2022

Published: 5 December 2022

Publisher's Note: MDPI stays neutral with regard to jurisdictional claims in published maps and institutional affiliations.



Copyright: © 2022 by the authors. Licensee MDPI, Basel, Switzerland. This article is an open access article distributed under the terms and conditions of the Creative Commons Attribution (CC BY) license (<https://creativecommons.org/licenses/by/4.0/>).

Keywords: digital twin; metaverse; reverse auction; resource allocation

1. Introduction

In recent years, different industries and government sectors have focused on metaverses in the context of the global coronavirus epidemic [1–3]. The metaverse can provide users with an immersive virtual experience similar to the real world. Furthermore, developments in communication networks such as 5G and 6G have made the realization of the metaverse imaginable [4]. The structure of the metaverse can be divided into three layers: the physical layer, the virtual layer, and the technology layer, which includes technologies such as digital twin, blockchain, network communication, virtual reality (VR), augmented reality, and others.

Digital twin technology is valuable in a wide range of application scenarios and is crucial to the creation of the metaverse. For example, digital twin technology can be used to create a virtual environment of relevant teaching content so that students can immersively experience the content to strengthen their understanding and mastery [5].

Over 4300 English conversational scenarios have already been converted by the language learning platform Hoodoo Labs [6]. Thus, the platform enables users to enhance their English through immersive learning wherever they go. Another example is the optimization of industrial structures in factories using digital twin technology [7]. For instance, users can map plant structures, production line layouts, production processes, equipment, and other plant facilities, as well as operational layouts, to the metaverse in real time using digital twin technology when building a smart factory. Workers can then adjust the factory production line, equipment layout, and staffing in the metaverse. Finally, the productivity is verified after adjusting the structure to find the configuration that makes the factory the most productive. The metaverse enables faster, better adjustment of the plant's industrial structure while avoiding revenue loss from incorrect adjustments to the industrial structure. Another example can be seen in the field of smart cities, where users can use digital twin technology to map real-world cities to the virtual world in real time [8]. Specifically, to create a virtual city, a virtual service provider uses digital twin technology to digitize a series of real-world physical objects, including roads, urban buildings, vehicles, and pedestrians. Furthermore, simulated experiments can be performed by businesses and researchers in virtual cities. Simulated experiments in the virtual world, such as testing autonomous driving [9] and smart parking [10], are not only free of high risks but also result in the same experience as experimenting in the physical world. The construction of real-world virtual environments by virtual service providers (VSPs) using digital twin technology requires real-world data information transmitted by IoT devices. The VSP models a city in the real world to construct a smart city; however, it demands multiple base stations to receive the real-world data collected by IoT devices due to the scale of the physical city and the number of IoT devices collecting real-world data.

1.1. Motivation

Utilizing digital twin technology to construct virtual environments of the real world is only the first step in achieving the aforementioned goals. To construct a virtual environment of the real world, the VSP requires base stations to receive data from IoT devices. However, it can be difficult or expensive to build base stations in some remote locations. For example, if we want to build virtual environments of remote natural landscapes so that users can experience nature immersively at home, building base stations in natural landscapes to receive data from IoT devices is not feasible to achieve this purpose. Such an approach would be disruptive to the local environment and expensive. Moreover, we may not collect environmental data to update the virtual environment for a long time after the virtual environment has been built. Additionally, this will result in long periods of base station inactivity and no additional revenue. Therefore, we can use UAV base stations in place of traditional base stations to receive data from IoT devices [9]. We can place IoT devices that collect environmental data in various regions of an area to collect comprehensive environmental data. However, as the coverage area of UAV base stations is smaller than that of traditional base stations and the coverage area of natural scenic areas is large, a single UAV base station may not be able to cover the range of all IoT devices. Hence, we must send multiple UAV base stations to the area to provide resources for IoT devices so that the IoT devices can transmit data through the UAV base stations to the VSP to build the virtual environment. UAVs as base stations to receive data from IoT devices have the advantages of low environmental requirements, low cost, and the flexibility to move around as often as necessary. With these benefits of UAV base stations (UAV-BSs), the VSP can also use a number of UAV base stations in a metaverse application scenario such as smart cities (Figure 1) to receive data about the real world from IoT devices and use it to create a virtual representation of the real world. However, allocating resources of multiple base stations is challenging. IoT devices may be in the signal range of several base stations simultaneously, and they can transmit data information through different base stations. However, since the cost of communication between different base stations and IoT devices differs, the resources provided by different base stations, such as channel capacity and

number of channels, differ. Therefore, while creating a metaverse virtual environment, it is challenging to reasonably allocate the resources of several base stations to IoT devices.

This paper studies the problem of a VSP allocating multibase station wireless resources for IoT devices from the perspective of resource allocation when constructing a metaverse. Research on the metaverse is still in its infancy since it serves as a paradigm for next-generation networks, and only a very small amount of research has been focused on the problem of wireless resource distribution in the metaverse. In [9], the authors researched the problem of allocating channel resources to IoT devices to transmit data from a single UAV base station (UAV-BS) sent by a VSP to build a virtual representation of the physical world. In contrast to existing research, our work focuses on solving the problem of allocating resources to IoT devices from multiple UAV-BSs of VSP. We should fully utilize existing IoT devices, such as autonomous vehicles and smartphones, to transmit data to the VSP. VSP sends UAV-BSs to a specified area to build a metaverse virtual environment. Then, a winner set is selected by the VSP based on the parameters reported by IoT devices; finally, the VSP allocates UAV-BS resources to the winner set. The problem of limited base station resources has led to multiple IoT devices competing for resources. However, in our hypothesis, IoT devices may belong to third parties (e.g., autonomous vehicles), so to enable themselves to be the winners, they may misrepresent their parameters to the VSP and manipulate the results of VSP resource allocation. To ensure the quality of VSP services, we must design mechanisms to ensure a reasonable resource allocation result.



Figure 1. Smart City Diagram.

1.2. Contribution

This paper solves the problem of metaverse multibase station resource allocation based on the principle of the reverse auction mechanism to ensure the quality of service of the VSP. Our main contributions are as follows:

1. We have built a metaverse digital twin application framework, a three-layer architecture that includes IoT devices, UAV-BSs, and VSP platforms. Additionally, the problem of competitive channel resource allocation is converted into an integer programming model with constraints. The objective is to enable the VSP to reasonably allocate base station resources when building a metaverse and to enable the whole model to achieve greater social welfare (the sum of IoT device utility and VSP utility).
2. We design the optimal reverse auction mechanism based on the optimal allocation and VCG mechanism to solve the problem of IoT devices competing for base station resources. However, as the resource allocation problem is NP-hard, it cannot be

solved in polynomial time. We also designed the metaverse digital twin resource allocation and pricing (MDTRAP) mechanism based on monotonic allocation and key value theory. Specifically, the MDTRAP mechanism includes an allocation algorithm (MDTRAP_ALLOC) to calculate the result of base station resource allocation when the number of IoT devices and base station scale are large and a payment algorithm (MDTRAP_PAY) to calculate the payment scheme. Both mechanisms are compared in terms of social welfare, the number of winners, total payments, and so on. Meanwhile, we demonstrate that both mechanisms have incentive compatibility and individual rationality.

The remaining chapters of this paper are organized as follows. We discuss the existing research on metaverse and mechanism design in Section 2. We describe the problem of multiple base station resource allocation when constructing a metaverse using digital twin technology and propose a corresponding integer linear programming constraint model in Section 3. Meanwhile, we present preliminary work on auction mechanism design and propose a realistic optimal reverse auction mechanism. We design an auction mechanism and propose a corresponding resource allocation algorithm and an algorithm for calculating the price to be paid in Section 4. Then, we demonstrate that the mechanism has individual rationality and incentive compatibility. In Section 5, we experimentally evaluate two mechanisms and verify that the auction mechanism we designed can be used to solve the resource allocation for IoT devices by multiple base stations in the real world. Finally, in Section 6, we summarize our results and propose possible directions for future research.

2. Related Work

The metaverse, as a next-generation network, has many real-world application scenarios, which has led to many people researching it. Several current research directions related to the metaverse focus on (1) the problem of high standard requirements of the metaverse for networks [11,12], (2) metaverse data security problems [13,14] and (3) resource allocation problems involved in constructing metaverse frameworks [15,16], which is the main objective of our research.

A metaverse is a virtual world built as a representation of the real world, and the metaverse has a diverse demand for resources, which leads to the problem of the reasonable distribution of resources. To solve the uniform resource allocation problem under stochastic user demand, Ng et al. [15] proposed a stochastic optimal resource allocation scheme based on stochastic integer programming. To solve the online time-varying multidimensional resource allocation and pricing problem in the cloud, Zhang et al. [16] proposed a novel model of the time-varying multidimensional resource allocation problem and designed a realistic online auction mechanism. Chu et al. [17] developed an efficient framework based on semi-Markovian decision processes and proposed an intelligent access control algorithm to solve the problem of resource allocation in the metaverse. While related technologies such as cloud and edge computing have reduced the high standards demanded of networks by the metaverse, the heterogeneity of cloud and edge computing presents challenges to resource allocation and deployment constraints. Zhang et al. [18] proposed a cloud-side collaboration framework based on video live streaming services and used an auction mechanism to solve the resource competition problem among anchor users in live streaming services. In cloud computing environments, virtual machines are an important resource, making resource allocation for them a significant problem. Chen et al. [19] designed a genetic algorithm to solve the allocation problem. Nagpure et al. [20] proposed a dynamic resource allocation system to solve the problem of allocating virtual machine resources. How to rationally and reliably allocate resources to users in cloud computing is also a problem that remains to be solved. Alam et al. [21] proposed a heuristic algorithm to improve the reliability of resource allocation. Since the key to synchronizing the real world with the virtual world using digital twin technology is the data collected by IoT devices and sensors, Han et al. [22] used a hybrid evolutionary dynamics approach to design a dynamic resource allocation framework to synchronize a metaverse with IoT services and

data. The metaverse also has great potential in healthcare, Chengoden et al. [23] provided a comprehensive review of metaverse applications in healthcare, describing the latest technologies, potential procedures, and more. The above paper focuses on the problem of resource allocation in the metaverse domain; the difference from this paper is that this paper focuses on designing an auction mechanism to solve the problem of resource allocation of multiple base stations. The approaches used in the above papers did not use auctions to solve the resource allocation problem, while this paper uses auctions to solve the resource allocation and pricing problem.

With the emergence of technologies related to the metaverse, competition for data processing resources and bandwidth is inevitable; therefore, efficient methods of resource allocation, such as auction mechanism design, have drawn considerable attention from researchers. Zhang et al. [7] proposed two auction mechanisms for blockchain networks consisting of edge computing service providers and miners to solve the resource allocation and pricing problem in the vehicular network environment. Mobile data offloading is an effective way to reduce the burden on the network when building a metaverse. Therefore, Enfang et al. [24] designed a realistic incentive mechanism and proposed a data offloading auction greedy algorithm to select the most cost-effective bid. User demand for metaverse resources sometimes varies with time, so Zhang et al. [25] designed a policy-proof online auction mechanism to address the problem of time-varying resource allocation. When constructing virtual environments utilizing digital twin technology, a VSP requires data gathered by IoT devices or sensors for modeling. Lotfi et al. [9] proposed using semantic data instead of raw data for transmission and designed a reverse auction mechanism to solve the problem of IoT devices competing for single base station resources. The development of cloud computing has alleviated the network requirements of the metaverse, but cloud computing also aggregates a large number of online resources, such as virtual machines and CPUs. Xu et al. [26] proposed a resource allocation model based on a combined double auction mechanism to solve the resource allocation problem of cloud computing. Chichin et al. [27] proposed an adaptive greedy mechanism to help cloud providers allocate and price cloud resources. Zhang et al. [28] proposed a novel integer programming model for the time-varying batch VM allocation problem and designed two real auction mechanisms to solve the allocation and pricing problems in a competitive environment. Zaman et al. [29] designed an online mechanism for the dynamic configuration and allocation of virtual machines and resource pricing in the cloud. The above paper focuses on designing an auction mechanism to solve the problem of resource allocation and pricing in the metaverse domain. The difference from this paper is that this paper focuses on designing a reverse auction mechanism to solve the problem of multiple base station resource allocation and pricing when building a metaverse. While the above article uses a traditional auction approach to solve the problem of resource allocation and pricing between a single seller and multiple buyers, this paper uses a reverse auction approach to solve the problem of resource allocation and pricing between a single buyer and multiple sellers.

Some researchers have combined machine learning with mechanism design to solve problems in the field of resource allocation. Tra et al. [30] combined federated learning with an auction mechanism design to motivate users to join federated learning. Jiao et al. [31] proposed an auction-based market model to motivate users to participate in federated learning and developed an automated policy-proof mechanism based on deep reinforcement learning and graph neural networks to maximize social welfare. Lee et al. [32] proposed an edge computing model based on a bidding mechanism to handle machine learning code offloading. Zhu et al. [33] constructed a multilayer feedforward neural network to solve the resource allocation problem in wireless virtualization based on optimal auction design analysis. Although these studies combine machine learning with auction mechanism design and develop truthful auction mechanisms, the auction mechanisms in these studies are designed to maximize social welfare, and optimal resource allocation mechanisms that solve for optimal results with optimizers such as Cplex are not designed to be compared with these auction mechanisms. Moreover, this paper implements resource allocation and

pricing by designing an algorithm based on monotonic allocation and critical value, which can achieve resource allocation without excessive hardware support. Additionally, an optimal resource allocation mechanism is designed for comparison with the developed algorithm. The above papers combine the traditional auction approach with machine learning, which also ensures the maximization of social welfare, but it does not compare with the optimal resource allocation result. We use the reverse auction approach to solve the resource allocation problem, and the resource allocation result is approximate to the optimal result.

In summary, previous research about the metaverse has achieved good results. However, the main difference between this paper and existing research is that we study the multibase station channel resource allocation problem in a metaverse digital twin with an end-to-edge cloud three-layer framework and design a corresponding reverse auction mechanism to solve the resource allocation and pricing problem. Table 1 compares the research content of some articles in related work.

Table 1. Comparison of this paper with the related work.

Paper ID	Domain	Algorithm	Feature	Mechanism
Lotfi et al. [9]	Metaverse	Optimal	Single UAV base station, reverse auction	IR, IC
Zhang et al. [25]	Cloud	Optimal, critical value theory based	time-varying resource allocate	IR, Strategy-proof
Chichin et al. [27]	Cloud	Greedy	combinatorial auction	Truthfulness
Zaman et al. [29]	Cloud	Monotone, critical value theory based	Dynamic resource allocate, online mechanism	IR, IC
Tra et al. [30]	Wireless Cellular Networks	Machine-learning based	primal-dual greedy auction	IR, Truthfulness
Jiao et al. [31]	Wireless Federated Learning	Machine-learning based	approximate strategy-proof mechanism, automated strategy-proof mechanism based on deep reinforcement learning and graph neural networks	Truthfulness, IR
Zhu et al. [33]	Cellular network	Machine-learning based	multilayer feedforward neural network based on the analysis of optimal auction design	IR, IC, budget constraint
This paper	Metaverse	Optimal, Monotone, critical value theory based	Multiple UAV base stations, reverse auction	IR, IC

3. Multibase Station Resource Allocation in Metaverse Digital Twin and Mechanism Design Preliminary

Figure 2 shows the framework for constructing a metaverse digital twin application through multiple UAV-BSs. The VSP is responsible for building a virtual copy of the physical world using digital twin technology. After receiving data from IoT devices, the VSP utilizes digital modeling and other related technologies to organize the data and build a virtual copy of the real world and then continuously receives data from IoT devices to gradually improve the virtual environment through digital modeling technology. The IoT devices are responsible for collecting data from the real world environment, and the UAV-BS is responsible for allocating resources to the IoT devices to enable the IoT devices to transmit data to the VSP through the UAV-BS. In the figure, in the first step, IoT devices collect raw environmental data from the real-world environment. In the second step, IoT devices process the environmental data. For example, IoT devices can process collected environmental data through semantic extraction algorithms (FCN, Seg-Net), grayscale

processing or CNN. More importantly IoT devices transmit the value of the evaluated data collected to the VSP through the UAV-BS. The hypothesis that current IoT devices already have some data processing capability is reasonable [34]. In the third step, IoT devices report their parameters (number of channels requested, data value, and bid price) to the VSP. When constructing the metaverse, the VSP will select IoT devices based on data value and bid price; the higher the data value and the lower the bid price, the more likely that the IoT device will win. In the fourth step, the VSP selects IoT devices for the allocation of UAV-BSs resources; then, the IoT devices that become the winners transmit the processed environmental data to the VSP through UAV-BSs. In the fifth step, the VSP trains the model on the received data, obtains the model parameters, and constructs the virtual environment. In the sixth step, the VSP transmits the model parameters to IoT devices transmitting data through UAV-BSs (the parameters received by the IoT devices are the model parameters obtained from the VSP training the corresponding IoT device data) to update the original model parameters. In addition, IoT devices that are not winners receive the weighted aggregation of existing model parameters delivered by the VSP through UAV-BSs to update the original model parameters. One of the functions is to assess the value of the data collected by IoT devices in preparation for the next round of allocation. By continuing this process, the VSP can construct virtual environments realistically and quickly, and the model parameters used to evaluate data values will become increasingly accurate, facilitating the construction of virtual environments.

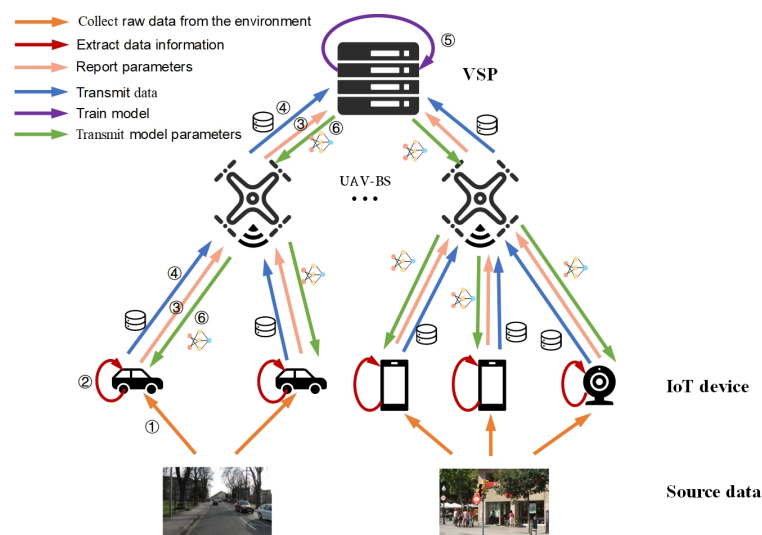


Figure 2. Constructing metaverse digital twin by receiving data from multiple UAV-BSs.

3.1. Service Cost and Data Value in Metaverse Digital Twin

When utilizing digital twin technology to construct a virtual environment for the considered application scenario, such as a smart city, the VSP must send several UAV-BSs to the area of interest to select IoT devices and receive the data sent by the selected IoT devices. As shown in Figure 2, the scenario includes a virtual service provider (VSP), a set of IoT devices $\mathcal{N} = \{1, \dots, N\}$ and several UAV base stations $\mathcal{M} = \{1, \dots, M\}$. In the resource allocation process, there are several indicators to calculate, such as the cost of IoT device services, the cost of data transmission, and the cost of channel usage.

1. Calculated cost: The cost c_i^{col} of collecting environmental data by IoT device i is defined as follows:

$$c_i^{col} = \sum_{k=1}^{m_i} d_{ik} \alpha_{ik} \quad (1)$$

where col represents the data collection phase of the IoT device, c_i^{col} is the calculated cost of IoT device i collecting real-world environmental data, m_i is the number of sensors on IoT device i , d_{ik} is the size of the data collected by sensor k of IoT device i

and α_{ik} is the unit cost of collecting real-world environmental data by sensor k of IoT device i . Table 2 shows some of the variables involved in the mechanism.

Table 2. Frequently used notations.

Variable	Description
\mathcal{M}	The set of UAV-BSs
\mathcal{N}	The set of IoT devices
c_i^{col}	The calculation cost of collecting environmental data by IoT device i
m_i	The number of sensors on IoT device i
d_{ik}	The data size collected by sensor k of IoT device i
α_{ik}	The unit cost for sensor k of IoT device i to collect real-world environmental data
c_i^{tra}	The calculation cost of IoT device i training raw data to extract data information
γ_i	The unit cost of IoT device i training raw data
λ_i	The data compression rate of IoT device i training raw data
c_{ij}^{comp}	The total cost of data transmission from IoT device i to VSP through UAV base station j
d_i^{tra}	The data size of IoT device i after training raw data
μ_j	The channel capacity of UAV-BS j
β_{ij}	The unit transmission cost between UAV-BS j and IoT device i
ch_{ij}	The number of channels requested by IoT device i to UAV-BS j
c_{ij}^{comm}	The communication cost of IoT device i transmitting data to VSP through UAV-BS j
c_{ij}^{total}	The total service cost of IoT device i transmitting data to VSP through UAV-BS j
c^{req}	The cost of UAV-BS requesting channels from wireless service provider
κ_j	The channel cost per unit allocation by wireless service provider to UAV-BS j
b_{ij}	The bid of IoT device i transmitting data through UAV-BS j
θ_i	The parameter reported by IoT device i to transmit data to VSP
V_i	The data information value of IoT device i
CH_j	The total number of channels of UAV-BS j
p_{ij}	The amount paid by VSP to IoT device i transmitting data through UAV-BS j
u_{ij}	The utility of IoT device i transmitting data to VSP through UAV-BS j
\hat{u}	The utility of VSP
x_{ij}	$\in \{0,1\}$, the decision variable, if its value is 1, it indicates that the IoT device i is allocated resources by the UAV base station j
$S(x)$	The social welfare of the whole system when the selected IoT device set is x

Since raw data must be processed first by IoT devices (e.g., grayscale processing, feature extraction), the calculated cost c_i^{tra} of training on raw data by IoT device i to extract data information is defined as follows:

$$c_i^{tra} = \gamma_i \sum_{k=1}^{m_i} d_{ik} \quad (2)$$

where tra represents the IoT device training raw data extraction data phase, c_i^{tra} is the calculated cost of the IoT device i training on collected raw data to extract data information, γ_i is the unit cost of the raw data collected by the IoT device i training. The total cost c_i^{comp} of data processing of the IoT device i is defined as follows:

$$c_i^{comp} = c_i^{col} + c_i^{tra} = \sum_{k=1}^{m_i} d_{ik} \alpha_{ik} + \gamma_i \sum_{k=1}^{m_i} d_{ik} \quad (3)$$

2. The communication cost of the IoT device transmitting data to the VSP via UAV-BS: After IoT devices train on the collected raw data, the size of the data is significantly decreased, and the size of the data after training is defined as follows:

$$d_i^{tra} = \lambda_i \sum_{k=1}^{m_i} d_{ik} \quad (4)$$

where *tra* represents the training data phase, d_i^{tra} is the size of the data obtained after training the raw data by IoT device *i*, and λ_i is the data compression rate of IoT device *i* training the raw data. The data transmitted by IoT device to the VSP are the data after training. For example, the IoT device can utilize the FCN algorithm to train the raw data and extract semantic data information such as the size, relative position, speed, weather condition, etc., of the objects in the raw data. Therefore, the communication cost of data transmission from IoT device *i* to VSP by UAV-BS *j* is defined as follows:

$$c_{ij}^{comm} = d_i^{tra} \beta_{ij} \quad (5)$$

where *comm* represents the cost of communication for IoT devices, c_{ij}^{comm} is the communication cost of IoT devices *i* transmitting data through UAV-BS *j* to the VSP. The total service cost of IoT device *i* to transmit data to the VSP through UAV base station *j* is the sum of (3) and (5), defined as follows:

$$\begin{aligned} c_{ij}^{total} &= c_i^{comp} + c_{ij}^{comm} \\ &= \sum_{k=1}^{m_i} d_{ik} \alpha_{ik} + \gamma_i \sum_{k=1}^{m_i} d_{ik} + d_i^{tra} \beta_{ij} \end{aligned} \quad (6)$$

where *total* represents the total cost of service.

3. Cost of UAV-BSs requesting channels from wireless service providers: Since wireless channel resources are provided by wireless service providers, UAV base stations have to request channels from wireless service providers for data transmission by IoT devices. IoT devices request the number of channels according to the size of the data after training, as follows:

$$ch_{ij} = d_i^{tra} / \mu_j \quad (7)$$

where ch_{ij} is the number of channels requested by IoT device *i* from UAV-BS *j* and μ_j is the channel capacity of UAV-BS *j*. Therefore, the cost of UAV-BSs requesting channels is defined as follows:

$$c^{chan} = \sum_{j=1}^{|\mathcal{M}|} \sum_{i=1}^{|\mathcal{N}|} \kappa_j x_{ij} ch_{ij} \quad (8)$$

where the channel allocation cost is different for each UAV base station due to distance. Therefore, κ_j is the unit allocation channel cost of wireless service providers to UAV-BSs. x_{ij} is a decision variable, where a value of 1 indicates that IoT device *i* is selected by UAV base station *j* to allocate resources; otherwise, the value is 0.

4. Data value: Data value is used to determine how much value an IoT device can bring to the VSP by the data that it is prepared to transmit and is an essential factor when the VSP makes allocation decisions. Data value is defined as follows:

$$v_i = f(d_i^{tra}) \quad (9)$$

where d_i^{tra} is the data after the IoT device has processed the collected raw data. The function *f* is a model parameter that the VSP delivers to the IoT device through the UAV-BS to evaluate the value of the data. The first delivered model parameters are those randomly generated by the VSP, but subsequent model parameters are obtained

by the VSP training the data that is transmitted by the IoT devices. For example, Ref. [35] proposed the application of CNN-based YOLOv3 for object recognition and image classification in autonomous vehicles, where we can transmit the algorithmic model back to the IoT device for classification, recognition, and value determination of newly collected data. For example, the more objects, such as vehicles and pedestrians, there are in the collected data and the more states of the collected objects (e.g., travel direction, travel speed, relative position), the greater the value of the data will be. This is because the more objects there are in the data, the easier it is for the virtual environment to restore real-world scenes and give the user a sense of being in real life. Additionally, more objects are more favorable for autonomous driving testing, smart parking and other scenarios. When the user can experience a variety of objects in the virtual environment that are in the real world, the user's sense of experience increases dramatically. Furthermore, more objects being copied in the virtual world will bring a greater challenge for autonomous driving testing, making the test results closer to those obtained in the real world. The more object states that are collected, the closer the virtual environment will be to the real world, which is beneficial for testing and simulation. For instance, a copy of a moving vehicle will give the user a more realistic experience than a copy of a stationary vehicle in a virtual environment and can also provide more diverse possibilities for autonomous driving testing. Therefore, when there are more objects and more states of objects in the data, the corresponding data value is greater. In another example [9], the real-world weather conditions in the data collected by IoT devices are an essential factor in evaluating the value of the data, and the worse the weather conditions are, the greater the value of the data. On the other hand, the data transmitted by the IoT device to the VSP are data after training, and the number of channels requested for data transmission is determined by the size of that data. For different IoT devices with the same raw data, the smaller the volume of data after training is, the more likely the IoT device will be the winner. Thus, the smaller the volume of data transmitted by the IoT device is, the greater its data value.

3.2. Social Welfare Maximization in Metaverse Digital Twin

In our designed model, there are \mathcal{N} sellers (IoT devices), \mathcal{M} UAV-BSs, and one buyer (VSP). A reverse auction method, contrary to the role of sellers and buyers in traditional auctions, is suitable for our designed model. Therefore, the VSP must conduct a reverse auction to select a set of IoT devices that will transmit data to the VSP through UAV base stations. Each IoT device bids a price at which it is willing to sell its data information to the VSP, and the bid is defined as the vector $\mathbf{b}_i = (b_{i1}, \dots, b_{ij}, \dots, b_{i|\mathcal{M}|})$, where b_{ij} represents the bid of IoT device i that transmits data through UAV-BS j . Since the channel resources provided by UAV base stations cannot satisfy the resource requests of all IoT devices, IoT devices must compete for the channel resources provided by UAV base stations. Define $\mathbf{ch}_i = (ch_{i1}, \dots, ch_{ij}, \dots, ch_{i|\mathcal{M}|})$ as the vector of the number of channels requested by IoT devices to UAV-BSs. IoT devices may change their bids to make themselves more profitable, so we design the auction with incentive-compatible properties to ensure that devices report their parameters truthfully. IoT devices do not have the same value of data information due to differences in the locations of the sensors, hardware specifications, machine learning algorithms on the IoT devices, etc. Therefore, in addition to the size of the data volume and the bids of IoT devices, the VSP must select IoT devices to transmit data to the VSP through the UAV-BS based on the value of the data information reported by the IoT devices. IoT device i reports parameter type $\theta_i = \{\mathbf{b}_i, \mathbf{ch}_i, v_i\}$, where v_i is the value of the data information. An IoT device can only be selected to be allocated channels by a single UAV-BS, i.e., the IoT device either becomes the winner and is allocated all the requested channels by a single UAV-BS or it becomes the loser and is not allocated channel resources. Meanwhile, UAV-BS j cannot be allocated more channels than the total number of channels it has, $CH_j, j \in \mathcal{M}$. In addition, the data information required by the VSP to build the virtual environment is characterized by timeliness, i.e., the selection of IoT devices

and the data transmitted should occur within a time threshold. Based on this setting, it is easy to design mechanisms of multiple rounds for real-time scenarios, but we focus on the problem of resource allocation for a single round.

The utility of the IoT device i is the difference between the amount p_{ij} paid by the VSP to IoT device i transmitting data through UAV-BS j and the bid b_{ij} of IoT device i transmitting data through UAV-BS j to the VSP. If IoT device i is not selected, then the utility is 0, as follows:

$$u_{ij} = \begin{cases} p_{ij} - b_{ij} & x_{ij} = 1 \\ 0 & x_{ij} = 0 \end{cases} \quad (10)$$

where b_{ij} and c_{ij}^{total} are equal in the case of true reporting by IoT device i . The utility of the VSP is the data value of the IoT devices in the set of winners minus the amount paid by the VSP to the IoT devices that become winners minus the cost of the UAV base station to request channel allocation from the wireless service provider. The definition is as follows:

$$\hat{u} = \sum_{j=1}^{|\mathcal{M}|} \sum_{i=1}^{|\mathcal{N}|} x_{ij} v_{ij} - \sum_{j=1}^{|\mathcal{M}|} \sum_{i=1}^{|\mathcal{N}|} x_{ij} p_{ij} - c^{chan} \quad (11)$$

where x_{ij} is a binary decision variable whose value of 1 indicates that IoT device i is selected by the UAV-BS j to allocate channels to transmit data to the VSP ($x_{ij} = 1$) and is otherwise 0 ($x_{ij} = 0$). The social welfare of the whole system is the sum of the utilities of all participating entities, including the VSP and IoT devices, as follows:

$$\begin{aligned} S(\mathcal{X}) &= \hat{u} + \sum_{j=1}^{|\mathcal{M}|} \sum_{i=1}^{|\mathcal{N}|} x_{ij} u_{ij} \\ &= \sum_{j=1}^{|\mathcal{M}|} \sum_{i=1}^{|\mathcal{N}|} x_{ij} v_{ij} - \sum_{j=1}^{|\mathcal{M}|} \sum_{i=1}^{|\mathcal{N}|} x_{ij} b_{ij} - \sum_{j=1}^{|\mathcal{M}|} \sum_{i=1}^{|\mathcal{N}|} \kappa_j x_{ij} c_{ij} \end{aligned} \quad (12)$$

Our objective is to solve the social welfare maximization problem, which can be transformed into an integer linear programming problem with constraints, defined as follows:

$$\max S = \sum_{j=1}^{|\mathcal{M}|} \sum_{i=1}^{|\mathcal{N}|} x_{ij} v_{ij} - \sum_{j=1}^{|\mathcal{M}|} \sum_{i=1}^{|\mathcal{N}|} x_{ij} b_{ij} - \sum_{j=1}^{|\mathcal{M}|} \sum_{i=1}^{|\mathcal{N}|} \kappa_j x_{ij} c_{ij} \quad (13a)$$

$$\text{Subject to: } \sum_{i \in \mathcal{N}} x_{ij} c_{ij} \leq CH_j, \forall j \in \mathcal{M} \quad (13b)$$

$$\sum_{j \in \mathcal{M}} x_{ij} \leq 1, \forall i \in \mathcal{N} \quad (13c)$$

$$x_{ij} \in \{0, 1\}, \forall i \in \mathcal{N}, \forall j \in \mathcal{M} \quad (13d)$$

where Formula (13a) represents maximizing social welfare. Social welfare is the data information value of the IoT devices that become the winners minus the bid of the IoT devices that become the winners minus the cost of the UAV-BSs requesting channels from the wireless service providers. The above integer linear programming problem enables the model we have designed to obtain the maximum benefit. Formula (13b) indicates that UAV-BS j allocates no more channel resources to its selected IoT devices than the total number of channel resources it provides itself. Formula (13c) indicates that each IoT device can be allocated channel resources by at most a single UAV-BS. Formula (13d) indicates that the problem is an integer linear programming problem. In a social welfare maximizing reverse auction mechanism, the resource allocation problem is first solved, after which the amount to be paid by the VSP to the IoT devices in the set of winners is calculated, subject to the outcome of the allocation being determined.

3.3. Optimal VCG Reverse Auction Mechanism Design in Metaverse Digital Twin

VCG is an auction mechanism for payment calculation based on the optimal allocation solution, which can be solved by the Cplex solver to obtain the optimal allocation result. We have designed the payment rule based on the VCG mechanism as follows:

$$p_{ij} = \begin{cases} S(\mathcal{X}^*) - S(\mathcal{X}_{-i}^*) + b_{ij}x_{ij} & x_{ij} = 1 \\ 0 & x_{ij} = 0 \end{cases} \quad (14)$$

where p_{ij} is the amount paid by the VSP to IoT device i that transmits data to the VSP through UAV-BS j . \mathcal{X}^* is the set of IoT device winners in the case of maximizing social welfare. $S(\mathcal{X}^*)$ represents the social welfare achieved by the model when the set of winners is \mathcal{X}^* . \mathcal{X}_{-i}^* is the set of IoT device winners when social welfare is maximized after the exclusion of IoT device i . $S(\mathcal{X}_{-i}^*)$ represents the social welfare achieved by the model when the set of winners is \mathcal{X}_{-i}^* . Clearly, $S(\mathcal{X}^*) \geq S(\mathcal{X}_{-i}^*)$; thus, if user i wins, $p_{ij} = S(\mathcal{X}^*) - S(\mathcal{X}_{-i}^*) + b_{ij} \geq b_{ij}$.

Theorem 1. *The optimal VCG reverse auction mechanism is incentive compatible.*

Proof. Since in the system, channel parameter \mathbf{ch}_i and data value parameter v_i are calculated by IoT devices or sensors, we do not consider the possibility of fake values of these two parameters. Therefore, we only consider the case where bid \mathbf{b}_i is fake.

When IoT device k is truthfully reporting parameters, its utility is defined as follows:

$$u_{kj} = p_{kj} - b_{kj} = S(\mathcal{X}^*) - S(\mathcal{X}_{-k}^*) \quad (15)$$

When IoT device k does not bid truthfully, its utility is defined as follows:

$$\begin{aligned} u'_{kj} &= p'_{kj} - x_{kj}b_{kj} \\ &= S(\mathcal{X}) - S(\mathcal{X}_{-k}) + x_{kj}b'_{kj} - x_{kj}b_{kj} \\ &= \left[\sum_{j=1}^{|\mathcal{M}|} \sum_{i=1}^{|\mathcal{N}|} x_{ij}v_i - \left(\sum_{j=1}^{|\mathcal{M}|} \sum_{i=1, i \neq k}^{|\mathcal{N}|} x_{ij}b_{ij} + x_{kj}b'_{kj} \right) - \sum_{j=1}^{|\mathcal{M}|} \sum_{i=1}^{|\mathcal{N}|} \kappa_j x_{ij}ch_{ij} \right] \\ &\quad - \left[\sum_{j=1}^{|\mathcal{M}|} \sum_{i=1, i \neq k}^{|\mathcal{N}|} x'_{ij}v_i - \sum_{j=1}^{|\mathcal{M}|} \sum_{i=1, i \neq k}^{|\mathcal{N}|} x'_{ij}b_{ij} - \sum_{j=1}^{|\mathcal{M}|} \sum_{i=1, i \neq k}^{|\mathcal{N}|} \kappa_j x'_{ij}ch_{ij} \right] \\ &\quad + x_{kj}b'_{kj} - x_{kj}b_{kj} \end{aligned} \quad (16)$$

where b'_{kj} is the bid of IoT device i that transmits data to the VSP through UAV-BS j ($b'_{kj} \neq b_{kj}$). $S(\mathcal{X}_{-k}^*)$ and $S(\mathcal{X}_{-k})$ are the maximum social welfare of the system after excluding IoT devices k , which leads to $S(\mathcal{X}_{-k}^*) = S(\mathcal{X}_{-k})$. The difference between u'_{kj} and u_{kj} is therefore defined as follows:

$$\begin{aligned}
u'_{kj} - u_{kj} &= S(\mathcal{X}) - S(\mathcal{X}_{-k}) + x_{kj}b'_{kj} - x_{kj}b_{kj} - S(\mathcal{X}^*) + S(\mathcal{X}^*_{-k}) \\
&= S(\mathcal{X}) + x_{kj}b'_{kj} - x_{kj}b_{kj} - S(\mathcal{X}^*) \\
&= \left[\sum_{j=1}^{|\mathcal{M}|} \sum_{i=1}^{|\mathcal{N}|} x_{ij}v_i - \left(\sum_{j=1}^{|\mathcal{M}|} \sum_{i=1, i \neq k}^{|\mathcal{N}|} x_{ij}b_{ij} + x_{kj}b'_{kj} \right) - \sum_{j=1}^{|\mathcal{M}|} \sum_{i=1}^{|\mathcal{N}|} \kappa_j x_{ij}ch_{ij} \right] \\
&\quad - \left[\sum_{j=1}^{|\mathcal{M}|} \sum_{i=1}^{|\mathcal{N}|} x_{ij}^*v_i - \sum_{j=1}^{|\mathcal{M}|} \sum_{i=1}^{|\mathcal{N}|} x_{ij}^*b_{ij} - \sum_{j=1}^{|\mathcal{M}|} \sum_{i=1}^{|\mathcal{N}|} \kappa_j x_{ij}^*ch_{ij} \right] + x_{kj}b'_{kj} - x_{kj}b_{kj} \\
&= \left[\sum_{j=1}^{|\mathcal{M}|} \sum_{i=1}^{|\mathcal{N}|} x_{ij}v_i - \sum_{j=1}^{|\mathcal{M}|} \sum_{i=1, i \neq k}^{|\mathcal{N}|} x_{ij}b_{ij} - \sum_{j=1}^{|\mathcal{M}|} \sum_{i=1}^{|\mathcal{N}|} \kappa_j x_{ij}ch_{ij} \right] \\
&\quad - \left[\sum_{j=1}^{|\mathcal{M}|} \sum_{i=1}^{|\mathcal{N}|} x_{ij}^*v_i - \sum_{j=1}^{|\mathcal{M}|} \sum_{i=1}^{|\mathcal{N}|} x_{ij}^*b_{ij} - \sum_{j=1}^{|\mathcal{M}|} \sum_{i=1}^{|\mathcal{N}|} \kappa_j x_{ij}^*ch_{ij} \right] \\
&\quad - x_{kj}b'_{kj} + x_{kj}b'_{kj} - x_{kj}b_{kj} \\
&= \left[\sum_{j=1}^{|\mathcal{M}|} \sum_{i=1}^{|\mathcal{N}|} x_{ij}v_i - \left(\sum_{j=1}^{|\mathcal{M}|} \sum_{i=1, i \neq k}^{|\mathcal{N}|} x_{ij}b_{ij} + x_{kj}b_{kj} \right) - \sum_{j=1}^{|\mathcal{M}|} \sum_{i=1}^{|\mathcal{N}|} \kappa_j x_{ij}ch_{ij} \right] \\
&\quad - \left[\sum_{j=1}^{|\mathcal{M}|} \sum_{i=1}^{|\mathcal{N}|} x_{ij}^*v_i - \sum_{j=1}^{|\mathcal{M}|} \sum_{i=1}^{|\mathcal{N}|} x_{ij}^*b_{ij} - \sum_{j=1}^{|\mathcal{M}|} \sum_{i=1}^{|\mathcal{N}|} \kappa_j x_{ij}^*ch_{ij} \right] \\
&= \left[\sum_{j=1}^{|\mathcal{M}|} \sum_{i=1}^{|\mathcal{N}|} x_{ij}v_i - \sum_{j=1}^{|\mathcal{M}|} \sum_{i=1}^{|\mathcal{N}|} x_{ij}b_{ij} - \sum_{j=1}^{|\mathcal{M}|} \sum_{i=1}^{|\mathcal{N}|} \kappa_j x_{ij}ch_{ij} \right] \\
&\quad - \left[\sum_{j=1}^{|\mathcal{M}|} \sum_{i=1}^{|\mathcal{N}|} x_{ij}^*v_i - \sum_{j=1}^{|\mathcal{M}|} \sum_{i=1}^{|\mathcal{N}|} x_{ij}^*b_{ij} - \sum_{j=1}^{|\mathcal{M}|} \sum_{i=1}^{|\mathcal{N}|} \kappa_j x_{ij}^*ch_{ij} \right] \leq 0
\end{aligned} \tag{17}$$

After derivation, the result of the difference between the two in Formula (17) is the difference in social welfare achieved by the different sets of winners, with both bids being truthful. However, \mathcal{X}^* is the optimal set of IoT devices that maximizes social welfare obtained using the solver, so there will always be $u'_{kj} - u_{kj} \leq 0$. Hence, there is no incentive for IoT devices to fake their bids. This shows that the auction mechanism we designed has the property of incentive compatibility. \square

Theorem 2. *The optimal VCG reverse auction mechanism is individually rational.*

Proof. Considering that the mechanism is truthful, Formula (15) shows that:

$$\begin{aligned}
u_{kj} &= S(\mathcal{X}^*) - S(\mathcal{X}^*_{-k}) \\
&= \left(\sum_{j=1}^{|\mathcal{M}|} \sum_{i=1}^{|\mathcal{N}|} x_{ij}^*v_i - \sum_{j=1}^{|\mathcal{M}|} \sum_{i=1}^{|\mathcal{N}|} x_{ij}^*b_{ij} - \sum_{j=1}^{|\mathcal{M}|} \sum_{i=1}^{|\mathcal{N}|} \kappa_j x_{ij}^*ch_{ij} \right) \\
&\quad - \left(\sum_{j=1}^{|\mathcal{M}|} \sum_{i \neq k}^{|\mathcal{N}|} x_{ij}^*v_i - \sum_{j=1}^{|\mathcal{M}|} \sum_{i \neq k}^{|\mathcal{N}|} x_{ij}^*b_{ij} - \sum_{j=1}^{|\mathcal{M}|} \sum_{i \neq k}^{|\mathcal{N}|} \kappa_j x_{ij}^*ch_{ij} \right) \geq 0
\end{aligned} \tag{18}$$

Since \mathcal{X}^* is the set of IoT devices that maximize social welfare obtained using the solver and \mathcal{X}^*_{-k} is the set of IoT devices that maximize social welfare obtained using the solver after excluding IoT device k , we know that $S(\mathcal{X}^*) \geq S(\mathcal{X}^*_{-k})$. Therefore, for $u_{kj} \geq 0$, IoT devices can obtain nonnegative utility by participating in this auction mechanism. In summary, the auction mechanism we designed has the property of individual rationality.

However, the optimal allocation problem in the optimal mechanism is NP-hard and cannot be solved in polynomial time, so we must design a mechanism that is more computationally efficient. \square

4. Metaverse Digital Twin Resource Allocation and Pricing (MDTRAP) Mechanism

In this section, our main contribution is the design of a truthful auction mechanism based on monotonic allocation and critical value to solve the resource allocation problem for multiple base stations in the metaverse digital twin. Specifically, the allocation of base station resources based on the price per unit of data value significantly reduces the time for the VSP to select IoT devices for allocation of base station resources, and the payment algorithm we design enables the VSP to pay the IoT devices less, which is beneficial to the VSP.

4.1. High-Level Idea

4.1.1. Price Per Unit of Data Value

The advantage of price per unit of data value in the mechanism we designed is that it clearly reflects the price that each IoT device expects for the data value it provides, thus allowing the VSP to reasonably allocate resources based on the price per unit of data value and improving the overall social welfare.

For $i \in \mathcal{N}, j \in \mathcal{M}$, the price per unit of data value bv_{ij} is defined as follows:

$$bv_{ij} = \frac{b_{ij}}{v_i}, \forall i \in \mathcal{N}, \forall j \in \mathcal{M} \quad (19)$$

where b_{ij} is the bid of IoT device i that transmits data to the VSP through UAV-BS j and v_i is the data value of IoT device i , which is evaluated by the parameters of the trained model.

4.1.2. Allocation Strategy

For $i \in \mathcal{N}, j \in \mathcal{M}$, the request information of devices is sorted in nondecreasing order according to the price per unit of data value. Then, the VSP determines the corresponding IoT device and UAV base station according to the nondecreasing set and allocates the resources of that UAV-BS to that IoT device. We think this allocation strategy is reasonable. The VSP needs the data collected by the IoT devices to build the virtual environment of the metaverse, and the more value the data collected by the IoT devices have, the more beneficial it is for the VSP to build the metaverse. However, as the resources are limited, the VSP can only allocate base station resources to some IoT devices. In real application scenarios, some IoT devices have high data value but their bids are too high. If only the data value of the IoT devices is considered, the VSP may obtain less revenue by selecting these IoT devices. Therefore, for the VSP to select IoT devices with greater data value and lower bids and for the whole system to achieve greater social welfare, a reasonable strategy is to select devices according to the nondecreasing order of price per unit of data value.

4.2. The Framework of MDTRAP

MDTRAP is a framework applied to metaverse digital twin multibase station resource allocation. MDTRAP is invoked when the VSP needs data collected by IoT devices to build or update the metaverse virtual environment and is used to help the VSP select the IoT devices to allocate base station resources and to pay price calculations. MDTRAP includes the resource allocation algorithm (MDTRAP_ALLOC) and the price paid algorithm (MDTRAP_PAY). Algorithm 1 represents the framework of the MDTRAP mechanism.

The framework we designed is divided into two phases: the allocation phase (solved by the MDTRAP_ALLOC algorithm) and the payment phase (solved by the MDTRAP_PAY algorithm). The MDTRAP_ALLOC algorithm can solve Formula (13a) and satisfy the corresponding constraints to obtain the assignment result. The MDTRAP_PAY algorithm can calculate the price paid based on critical value theory.

The inputs of the algorithm are the number **CH** of channels provided by all base stations, the value **v** of all IoT device data information, the bid **b** and the number **ch** of transmission data channels requested by the IoT devices to the UAV base stations, the set \mathcal{N} of IoT devices, and the set \mathcal{M} of UAV base stations. The outputs of the algorithm are the result \mathcal{X} of the base station resource allocation, the social welfare S of the system, and the payment scheme \mathcal{P} of the VSP. Line 1 is where the parameters are passed into the MDTRAP_ALLOC allocation algorithm to obtain the base-station resource allocation result \mathcal{X} of the system, the social welfare S and the combination (i^{lose}, j^{lose}) of device and base-station that has the lowest price per unit of data value in the set of losers. Line 2 is where the parameters are passed into the MDTRAP_PAY payment algorithm to calculate the price to be paid by the VSP to the IoT devices.

Algorithm 1 Framework of MDTRAP

Input: **CH, v, b, ch, M, N**

Output: $\mathcal{X}, S, \mathcal{P}$

- 1: $\mathcal{X}, S, i^{lose}, j^{lose} \leftarrow \text{MDTRAP_ALLOC}(\mathbf{CH}, \mathbf{v}, \mathbf{b}, \mathbf{ch}, \mathcal{M}, \mathcal{N})$
 - 2: $\mathcal{P} \leftarrow \text{MDTRAP_PAY}(\mathbf{v}, \mathbf{b}, \mathcal{X}, i^{lose}, j^{lose})$
 - 3: **return** $\mathcal{X}, S, \mathcal{P};$
-

4.3. MDTRAP_ALLOC Allocation Algorithm

The MDTRAP_ALLOC allocation algorithm (Algorithm 2) is used to solve the problem of IoT devices competing for base stations resources of the VSP. Line 1 initializes the variables $\mathcal{X}, \mathcal{X}', S, S', \mathcal{R}, \mathcal{D}, i^{lose}, j^{lose}$. Lines 2–7 calculate the price per unit of data value of the IoT devices and add them to set \mathcal{R} . This ratio is used to sort the combinations of IoT devices and base stations, and the combination with the smallest ratio is considered first as the winner. Line 8 is the set \mathcal{D} obtained by sorting the set \mathcal{R} in nondecreasing order. The nondecreasing sorting serves to facilitate the subsequent selection of the IoT device with the lowest price per unit of data value as the winner. Line 9 obtains element d in order from the set \mathcal{D} . The element with the lower price per unit of data value is preferred. Line 10 obtains the combination (i^{lose}, j^{lose}) of the IoT device and the UAV base station from d . Lines 11–15 are for determining whether IoT device i that transmits data to the VSP through UAV-BS j should be selected as the winner. Line 11 determines whether the remaining channels of UAV-BS j satisfy the channel request of IoT device i and whether IoT device i has been selected for channel allocation by the base station. The constraints (13b,b) are guaranteed. Line 12 assigns a value of 1 to the decision variable of the winner device, and this line together with line 11 guarantees constraint (13c). Line 13 determines the winning device for allocation. Line 14 continuously updates CH_j according to the winner set, and this line and line 11 together guarantee (13b). Line 16 calculates social welfare based on Formula (12) and the current set \mathcal{X}' of decision variables. Lines 17–24 compare the social welfare S to be output by the algorithm with the social welfare S' calculated above. If the condition is true, then S' is assigned to S and the decision variable \mathcal{X}' is assigned to \mathcal{X} . If the condition is false, then the current device and base station combination (i, j) is set to (i^{lose}, j^{lose}) and the loop is terminated. The objective function is guaranteed to be maximized.

Algorithm 2 MDTRAP_ALLOC**Input:** CH, \mathbf{v} , \mathbf{b} , \mathbf{ch} , \mathcal{M} , \mathcal{N} **Output:** \mathcal{X} , S , i^{lose} , j^{lose} .

```

1: Define  $\mathcal{X} = \emptyset, \mathcal{X}' = \emptyset, S = 0, S' = 0, \mathcal{R} = \emptyset, \mathcal{D} = \emptyset, i^{lose} = 0, j^{lose} = 0$ ;
2: for all  $i \in \mathcal{N}$  do
3:   for all  $j \in \mathcal{M}$  do
4:      $bv_{ij} \leftarrow b_{ij}/v_i$ 
5:      $\mathcal{R} \leftarrow \mathcal{R} \cup bv_{ij}$ 
6:   end for
7: end for
8:  $\mathcal{D} \leftarrow \text{nondecrease} - \text{sort}(\mathcal{R})$ 
9: for all  $d \in \mathcal{D}$  do
10:  get the combination (i, j) of IoT devices and BS from d
11:  if  $CH_j \geq ch_{ij}$  and  $\sum_{j=1}^{|\mathcal{M}|} x_{ij} < 1$  then
12:     $x_{ij} \leftarrow 1$ 
13:     $\mathcal{X}' \leftarrow \mathcal{X}' \cup x_{ij}$ 
14:     $CH_j \leftarrow CH_j - ch_{ij}$ 
15:  end if
16:   $S' \leftarrow \sum_{j=1}^{|\mathcal{M}|} \sum_{i=1}^{|\mathcal{N}|} x'_{ij} v_{ij} - \sum_{j=1}^{|\mathcal{M}|} \sum_{i=1}^{|\mathcal{N}|} x'_{ij} b_{ij} - \sum_{j=1}^{|\mathcal{M}|} \sum_{i=1}^{|\mathcal{N}|} \kappa_j x'_{ij} ch_{ij}$ 
17:  if  $S < S'$  then
18:     $S \leftarrow S'$ 
19:     $\mathcal{X} \leftarrow \mathcal{X}'$ 
20:  else
21:     $i^{lose} \leftarrow i$ 
22:     $j^{lose} \leftarrow j$ 
23:    break;
24:  end if
25: end for
26: return  $\mathcal{X}, S, i^{lose}, j^{lose}$ ;

```

4.4. MDTRAP_PAY Payment Algorithm

For the payment part of the MDTRAP mechanism, we borrow the threshold payment scheme from the greedy algorithm for data offloading auction (GAOA) in [24] and apply its improved version to our payment algorithm. We calculate the price paid by the VSP to the IoT device using an improved formula, as follows:

$$p_{ij} = \begin{cases} v_i \frac{b_{i^{lose} j^{lose}}}{v_{i^{lose}}} & x_{ij} = 1 \\ 0 & x_{ij} = 0 \end{cases} \quad (20)$$

where (i^{lose}, j^{lose}) is the combination of an IoT device and a base station that has the lowest price per unit of data value in the loser set.

The MDTRAP_PAY payment algorithm (Algorithm 3) is used to calculate the amount to be paid by the VSP to the IoT device, where the inputs to the algorithm are the data values \mathbf{v} of all IoT devices as well as the bids \mathbf{b} and the set \mathcal{X} of winners and the combination (i^{lose}, j^{lose}) of an IoT device and a base station that has the lowest price per unit of the data value in the loser set. The output of the algorithm is the payment scheme \mathcal{P} of the VSP. Line 1 initializes the set \mathcal{P} of prices paid. Lines 2–7 calculate the amount paid by the VSP to the IoT devices. Line 2 indicates that the loop continues as long as there are elements in the set \mathcal{X} of the winner. Line 3 is the device and base station combination (i, j) obtained from element x_{ij} of winner set \mathcal{X} . Line 4 is the calculation of the VSP payment amount based

on Formula (20). Line 5 is where the calculated payment amount p_{ij} is added to the set of payment prices \mathcal{P} . Line 6 removes the above IoT device from the set of winners.

Algorithm 3 MDTRAP_PAY

Input: $\mathbf{v}, \mathbf{b}, \mathcal{X}, i^{lose}, j^{lose}$

Output: \mathcal{P} .

```

1: Define  $\mathcal{P} = \emptyset$ ;
2: while  $|\mathcal{X}| > 0$  do
3:    $(i, j) \leftarrow$  according to element  $x_{ij}$  in set  $\mathcal{X}$ 
4:    $p_{ij} \leftarrow v_i \frac{b_{i^{lose}j^{lose}}}{v_{i^{lose}}}$ 
5:    $\mathcal{P} \leftarrow \mathcal{P} \cup p_{ij}$ 
6:    $\mathcal{X} \leftarrow \mathcal{X} \setminus i$ 
7: end while
8: return  $\mathcal{P}$ ;

```

4.5. Properties of the MDTRAP Mechanism

Theorem 3. The MDTRAP mechanism provides individual rationality.

Proof. The utility of IoT devices after inserting Formula (20) into Formula (10) is as follows:

$$\begin{aligned}
 u_{ij} &= p_{ij} - b_{ij} \\
 &= v_i \frac{b_{i^{lose}j^{lose}}}{v_{i^{lose}}} - b_{ij} \\
 &= v_i \left(\frac{b_{i^{lose}j^{lose}}}{v_{i^{lose}}} - \frac{b_{ij}}{v_i} \right)
 \end{aligned} \tag{21}$$

After derivation, the utility of IoT devices is as in Formula (21). $\frac{b_{ij}}{v_i}$ is the price per unit data value of IoT device i in the set of winners and $\frac{b_{i^{lose}j^{lose}}}{v_{i^{lose}}}$ is the minimum value of the price per unit data value in the set of losers. According to our design of the MDTRAP_ALLOC allocation algorithm, $\frac{b_{i^{lose}j^{lose}}}{v_{i^{lose}}} > \frac{b_{ij}}{v_i}$, therefore, $u_{ij} > 0$. With the algorithm we have designed, nonnegative utility can be obtained by IoT devices participating in the mechanism. Thus, the mechanism provides individual rationality. \square

Theorem 4. The MDTRAP mechanism provides incentive compatibility.

Proof.

1. $b_{ij} < b'_{ij}$: That is, IoT device i reports a high bid price, from which it follows that $bv_{ij} < bv'_{ij}$. We designed the MDTRAP_ALLOC allocation algorithm to select devices according to nondecreasing order of bv_{ij} .

(a) For the loser, it cannot become the winner by reporting a higher bid, and the utility is still 0.

(b) For the winner, if the device is still the winner after the high bid is reported, the amount paid by the VSP to the device is still $p_{ij} = v_i \frac{b_{i^{lose}j^{lose}}}{v_{i^{lose}}}$ and the utility

of the device is still $u_{ij} = p_{ij} - b_{ij} = v_i \frac{b_{i^{lose}j^{lose}}}{v_{i^{lose}}} - b_{ij}$. If the device becomes the loser after reporting a high bid, the amount paid by the VSP to the device is $p_{ij} = 0$, and the utility is $u_{ij} = 0$. As seen from the above two cases, an IoT device reporting a higher bid will not affect the amount paid to the device by the VSP, and the utility will not change. The IoT devices in the set of winners

face the risk of becoming losers by reporting high bids. Therefore, there is no incentive for IoT devices to report high bids.

2. $b_{ij} > b'_{ij}$: That is, IoT device i reports a low bid, and $bv_{ij} > bv'_{ij}$.
 - (a) For the winner, it is still the winner after reporting a low bid according to the MDTRAP_ALLOC allocation algorithm. The amount paid to that winner by the VSP is $p_{ij} = v_i \frac{b_{i \text{lose} j \text{lose}}}{v_{i \text{lose}}}$, and the utility of that winner is $u_{ij} = p_{ij} - b_{ij} = v_i \frac{b_{i \text{lose} j \text{lose}}}{v_{i \text{lose}}} - b_{ij}$. The above formulas show that reporting a low bid does not affect the amount paid by the VSP to the winning device and that the utility does not change.
 - (b) For the loser, if it is still the loser after reporting a low bid, the amount paid by the VSP to the device remains 0, and the utility is also 0. If the loser becomes the winner after reporting a low bid, in this case, $bv_{i \text{lose} j \text{lose}} > bv'_{ij}$, but in the real case $bv_{i \text{lose} j \text{lose}} < bv_{ij}$, which also leads to the amount paid by the VSP to the device being $p_{ij} = v_i \frac{b_{i \text{lose} j \text{lose}}}{v_{i \text{lose}}} < b_{ij}$, making the utility of the device $u_{ij} = p_{ij} - b_{ij} = v_i \frac{b_{i \text{lose} j \text{lose}}}{v_{i \text{lose}}} - b_{ij} < 0$. Therefore, there is no incentive for IoT devices to report low bids. In summary, the mechanism we have designed satisfies incentive compatibility.

□

Theorem 5. The time complexity of the MDTRAP mechanism is $O(MN \log(MN))$.

Proof. The time complexity of the double-layer loop of lines 1–7 in the MDTRAP_ALLOC algorithm is $O(MN)$. Line 8 utilizes a built-in sorting function with a time complexity of $O(MN \log(MN))$. The time complexity of the loop for lines 9–24 is $O(MN)$. Therefore, the time complexity of the MDTRAP_ALLOC algorithm is $O(MN \log(MN))$. The time complexity of lines 2–7 in the MDTRAP_PAY algorithm is less than $O(MN)$. Therefore, the time complexity of the MDTRAP mechanism is $O(MN \log(MN))$. □

5. Experimental Results

This paper compares the MDTRAP mechanism with the OPT-VCGRA mechanism and the first fit algorithm. The OPT-VCGRA mechanism is an algorithm that utilizes a Cplex solver to solve the problem model for optimal results, enabling the whole system to obtain the maximum social welfare. However, the OPT-VCGRA mechanism cannot obtain an optimal solution when the size of IoT devices and base stations is large. Therefore, this paper uses the OPT-VCGRA mechanism as a baseline. Four experiments are conducted on the number of channels, the number of IoT devices, the number of base stations, and the truthfulness of the mechanism. The experiments compare the two mechanisms in terms of several dimensions, such as total payment, social welfare, and the number of winners.

5.1. Experiment Setting

All experiments in this paper were run in an environment with Python version 3.7, and the experimental settings were as follows:

- Our original data came from the 2022 Huawei Software Elite Challenge [36]. We selected a subset of the data. Table 3 shows two data items from the Huawei Software Elite Challenge dataset. There are mtime and A–F items in the dataset, where mtime represents the time and A–F represent the bandwidth requested by clients A–F from the edge server at that time. We abstract the bandwidth as the size of the environmental data and select the bandwidth requested by Client A at different times as the size of the environmental data collected by different IoT devices. These available data were filtered for the size of the environmental data in [60, 120].

Table 3. Partial data from the Huawei Software Elite Challenge dataset.

mtime	A	B	C	D	E	F
2021-10-01 T00:00	261	259	440	33	235	497
2021-10-01 T00:05	13	13	2	4	10	61

- We assume that the unit cost of the sensors of IoT devices to collect real-world environmental data is the same and assume the unit cost $\alpha = 0.1$, in CNY/Mb. According to α and the size of the environmental data, we can calculate the cost of collecting environmental data by IoT devices. The cost sources for data collection by IoT devices include the cost of electricity and the cost of device consumption. The consumption of the device itself when collecting data is marginal. This design is reasonable considering the unit price of electricity and the power consumed by the device during the data collection phase.
- We assume equal data compression of the raw data for IoT device training and assume the data compression rate $\lambda = 0.1$. According to λ and the size of the environmental data, we can calculate the size of the data obtained after the IoT device has trained the raw data. This design is reasonable since in some processing algorithms (CNN, FCN), after processing the data, the data will be reduced to a tenth of the original size or less.
- We assume that the UAV-BSs have equal channel capacity and assume the channel capacity $\mu = 1$ Mbps. According to μ and the size of the data obtained after training the raw data by the IoT device, we can calculate the number of channels that the IoT device needs to request from the base stations. This design is reasonable because IoT devices transmit data to the VSP in Mb. To simplify the experiments, we assume the channel capacity $\mu = 1$ Mbps such that the size of the data to be transmitted by the device is equal to the number of channels requested.
- We select random numbers from a uniform distribution of $[0.5, 1]$ as the unit cost γ of training raw data from IoT devices in CNY/Mb. According to γ and the size of the environmental data, we can calculate the cost of training raw data for IoT devices. This design is reasonable because the cost of training raw data by IoT devices is related to power consumption, processing algorithms, and the size of the collected data. To balance the benefits of IoT devices and VSPs, we increase the value of unit cost γ slightly.
- We select random numbers from the uniform distribution of $[1, 6]$ as the unit data transmission cost β_{ij} of IoT devices, in CNY/Mb. According to β_{ij} and the size of the data after training, we can calculate the communication cost of an IoT device transmitting data to the VSP through the UAV base station. This design is reasonable because it reflects not only the difference in cost per unit of data transmission between IoT devices but also considers that the difference should not be too large, so the difference range is set to 5. In addition, the unit transmission cost must be realistic and the upper limit cannot be too large, so we must start with a smaller value, i.e., we set the lower limit to 1.
- We select random numbers from the uniform distribution of $[1, 3]$ as the cost κ of the UAV base stations to request channels from the wireless service providers, in CNY/Mb. According to κ and the number of channels requested by the IoT devices and the decision variables, we can calculate the cost of the channels requested by the UAV-BSs. The design is reasonable because it considers the pricing of wireless resource packages from major real-world providers and the pricing of other parts of the costs in the experiments.
- When generating bids, not only the cost of data transmission and calculation but also the degree to which users expect resources are considered. When calculating the bid price for each IoT device, we randomly draw a number in $[0, 1]$. When the number 0 is drawn, a random number is generated from a uniform distribution of $[0.5, 1]$. When the number 1 is drawn, a random number is generated from a uniform distribution of

[1,2]. We use the random number generated to represent the degree to which the user expects resources and later multiply the random number and the total cost (the sum of transmission and computational costs) to generate the bid of the user, simplifying the randomness of the bid of the user in the real world.

- In general, the more environmental data the IoT device collects, the greater the possibility that the data contain more information and the greater the corresponding data value. Therefore, to simplify the calculation of the data value, we assume that the data value is related to the size of the environmental data collected by the device. We use the ratio of the value of the environmental data volume to 5 as the data value of the IoT device to simplify the calculation of the data value in the real situation. This design is reasonable because the value of the data cannot be too small considering the total service costs of the IoT devices and the benefits to the VSP. Additionally, considering the value of the data in the actual situation, the value cannot be too large.
- We use the first fit algorithm as another method of comparison. The algorithm is another strategy to solve the resource allocation problem. In the allocation phase, the algorithm filters IoT devices based on the order in which they request resources from the base stations. The first fit algorithm verifies whether the IoT device has been selected by the base station for resource allocation when the base station resources can satisfy the requested resources of the IoT device. Then, the IoT device is allocated base station resources according to the order in which the IoT devices request resources. If the IoT device has already been selected for resource allocation by a base station, the request of the IoT device to other base stations is not considered (to ensure that the IoT device is selected for resource allocation by a single base station).

5.2. The Impact of the Number of Channels on Allocation

In the experiment, we verified the impact of the number of channels on the allocation results. The number of UAV-BSs $\mathcal{M} = 2$, the number of IoT devices $\mathcal{N} = 23$ and the total number of channels requested by IoT devices is 172. In this experiment, we assume that the unit of data to be transmitted by each IoT device is Mb. We compare the three algorithms in terms of social welfare, channel utilization, execution time, number of winners, and total payout dimensions for 20%, 40%, 60%, 80% and 100% of the total number of channels. The number of channels provided by the two UAV-BSs is equal in the five cases, 17, 35, 52, 68 and 86. The integer linear programming problem is solved deterministically by the Cplex solver, so we use the Cplex solver to calculate the optimal resource allocation results and maximum social welfare for the model and compare the results with those calculated using the MDTRAP mechanism and the first fit algorithm.

Figure 3a shows the social welfare of the three algorithms for different numbers of channels, where the OPT-VCGRA mechanism has the greatest social welfare because it calculates the social welfare from global considerations to obtain the optimal social welfare. Meanwhile, the social welfare solved by the MDTRAP mechanism is close to that of the OPT-VCGRA mechanism because the allocation algorithm of the MDTRAP mechanism selects IoT devices and base stations based on locally optimal aspects, maximizing social welfare. Once the number of channels exceeds 140, the social welfare obtained by both mechanisms is approximately the same. This is because when the number of channels provided by the UAV-BSs is greater than 140, the channel requests of most IoT devices can already be satisfied, so the social welfare obtained by both mechanisms is approximately the same. The first fit algorithm selects IoT devices based on the order in which they request resources, so the resulting social welfare is less than that calculated by the two mechanisms described above.

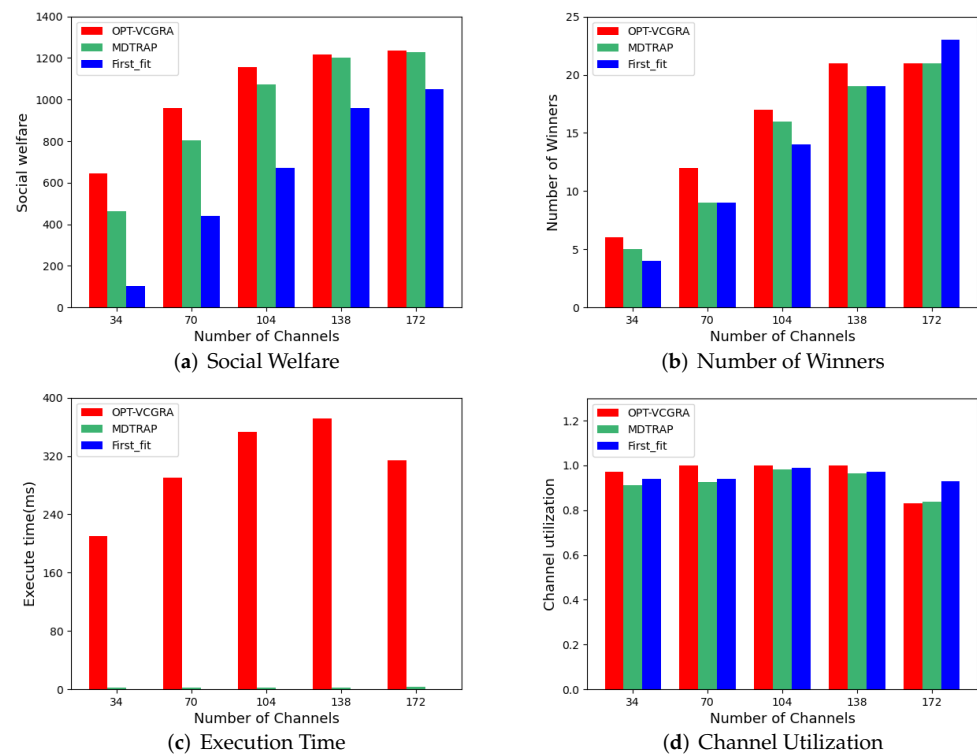


Figure 3. Social welfare, number of winners, algorithm execution time, and channel utilization under different numbers of channels.

Figure 3b represents the number of winners for the three algorithms under different numbers of channel resources. The difference in the number of winners for the three algorithms is small. The number of winners achieved by the first fit algorithm is greater than the number of winners achieved by both mechanisms at a channel count of 172, but both mechanisms prevail over the first adaptation algorithm in terms of social welfare. Although the number of channels provided by the base stations is equal to the number of device requests, because multiple base stations work together to provide resources and allocate them, when the base stations select some IoT devices, the remaining resources at each base station may not be able to satisfy the demand of the remaining devices. The first adaptation algorithm may select IoT devices with a low number of requested channels and low data value, resulting in a higher number of winners when the number of channels is 172 but lower social welfare. The number of winners calculated by the MDTRAP mechanism approximates that of the OPT-VCGRA mechanism, and the number of winners obtained by the MDTRAP mechanism is equal to that of the OPT-VCGRA mechanism when the number of channels is 172, but the social welfare is slightly less than that obtained by the OPT-VCGRA mechanism. This is because the OPT-VCGRA mechanism selects the set of winners that maximizes social welfare from a global perspective, which is why the time to solve for the optimal result with the Cplex solver increases rapidly when the numbers of IoT devices and UAV base stations increase. The MDTRAP mechanism, which selects IoT devices based on monotonically nondecreasing price per unit of data value, allocates resources from the local optimal perspective and thus falls somewhat short of the optimal outcome in terms of social welfare. In addition, the OPT-VCGRA mechanism results in the same number of winners when the number of channels increases from 138 to 172, with a slight increase in social welfare. This is because the remaining channels when the number of channels is 138 cannot meet the channel demand of some IoT devices with greater data information value, thereby resulting in selecting IoT devices with less channel demand and lower data information value. However, when the number of channels increases to 172, the remaining channels can meet the channel demand of IoT devices with more information

value, so to achieve the goal of maximizing social welfare, the original devices become losers and the IoT devices with more information value become winners.

Figure 3c represents the execution time of the three algorithms under different numbers of channels, where the OPT-VCGRA mechanism has the longest execution time, the MDTRAP mechanism has the second longest execution time that is much shorter than that of the OPT-VCGRA mechanism, and the first fit algorithm has the shortest execution time. This is because the first fit algorithm considers only the order in which IoT devices request resources, while the OPT-VCGRA mechanism considers each allocation result from the global optimum perspective and selects the allocation result that maximizes social welfare. Moreover, the MDTRAP mechanism calculates the resource allocation result from the local optimum perspective. The execution time of the OPT-VCGRA mechanism when the number of channels is 172 is less than that when the number of channels is 138 because when the channel resources are sufficient, the OPT-VCGRA mechanism performs less filtering of IoT devices and only those IoT devices that increase the social welfare are added to the winner set.

Figure 3d shows the channel utilization of the three algorithms under different numbers of channels. The channel utilization of the three algorithms is close to each other and close to 1. All three algorithms make the best possible use of channel resources, with the first fit algorithm achieving greater channel utilization than the two mechanisms when the number of channels is 172. This is because the first fit algorithm selects IoT devices to allocate as many channel resources as possible without considering social welfare.

Figure 4 represents the total amount paid by the VSP to the IoT device in both mechanisms under different numbers of channels. As the MDTRAP mechanism utilizes the key price to calculate the payment amount, the amount paid by the VSP in the MDTRAP mechanism is much smaller than that in the OPT-VCGRA mechanism. The OPT-VCGRA mechanism utilizes a payment algorithm based on the VCG mechanism, and Formula (14) is correlated with social welfare and bids, which results in higher amounts being paid by the VSP in the OPT-VCGRA mechanism. From the perspective of the VSP, it is a much better result that the MDTRAP mechanism can obtain higher data value with a lower payment, which is one of the advantages of the MDTRAP mechanism. A similar phenomenon was observed in subsequent experiments.

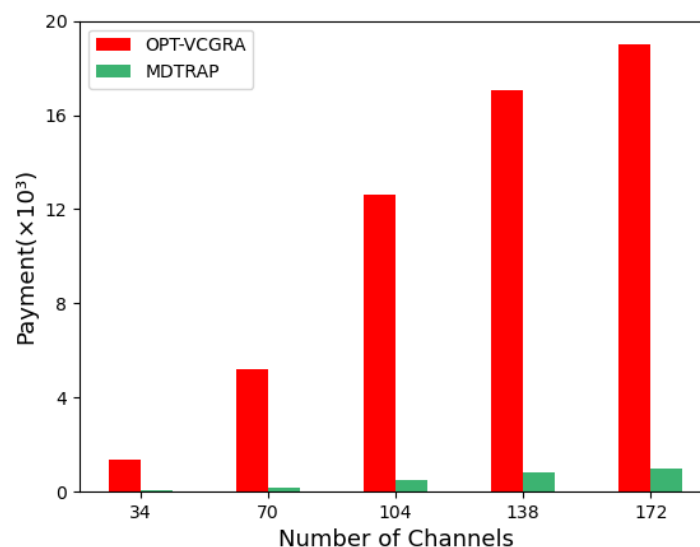


Figure 4. The total amount paid by the VSP to IoT devices under different numbers of channels.

5.3. The Impact of the Number of IoT Devices on Allocation

In this experiment, we verified the impact of IoT device size on allocation. The number of UAV-BSs $\mathcal{M} = 2$ and the number of IoT devices \mathcal{N} is 10, 50, 200, 500, and 1000, respectively. The total number of channels requested by IoT devices of the five

scales is 65, 413, 1650, 4125, and 8250, respectively. Meanwhile, we assume that the unit of data transmitted by the device is Mb. We consider that for real-world base stations, resources are limited and cannot satisfy the demands of all IoT devices. Therefore, in the experiment, we use 80% of the total number of channels to simulate the case of limited base station resources. The number of channels provided by the UAV base stations is equal, with the number of channels being 26, 165, 660, 1650, and 3300. In the experiment, we compare different aspects of the OPT-VCGRA mechanism, MDTRAP mechanism and first fit algorithm in the case of different numbers of IoT devices.

Figure 5a represents the social welfare of the three algorithms in the case of different numbers of IoT devices. The OPT-VCGRA mechanism has the highest social welfare, the MDTRAP mechanism is close to the OPT-VCGRA mechanism, and the first fit algorithm has the lowest social welfare. The OPT-VCGRA mechanism solves for the result that maximizes social welfare, but as the number of IoT devices increases, the OPT-VCGRA mechanism can no longer solve for the optimal result. The MDTRAP mechanism calculates a local optimum based on the price per unit of data value to maximize social welfare. The first fit algorithm selects devices according to only the order of resource requests, without considering social welfare. From the systemic perspective, obtaining greater social welfare under the same conditions is the better result.

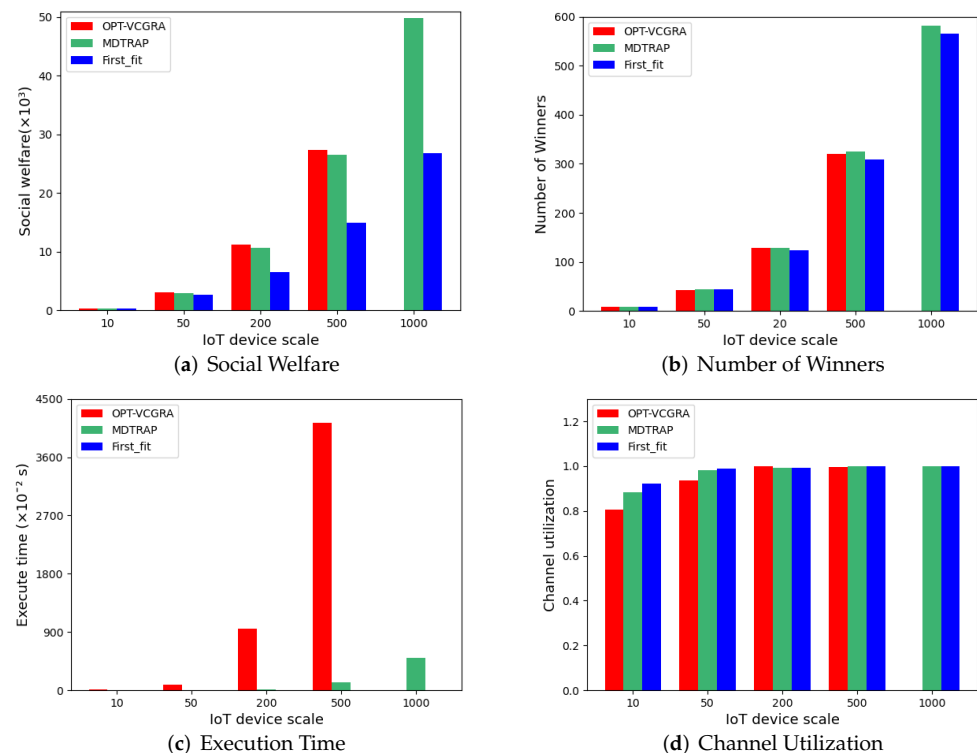


Figure 5. Social welfare, number of winners, execution time and channel utilization under different numbers of IoT devices.

Figure 5b represents the number of winners for the three algorithms in the case of different numbers of IoT devices. The three algorithms obtain a similar number of winners because most IoT devices have a similar demand for channel resources, but the data values and bids may differ significantly. Thus, the three algorithms obtain a similar number of winners under the same channel resources, but the social welfare differs substantially. Figure 5d represents the channel utilization of the three algorithms under different numbers of IoT devices. Since most IoT devices have a similar demand for channel resources and there is a similar number of winners for the three algorithms, the utilization of channel resources by the three algorithms is similar and close to 1.

Figure 5c represents the execution time of the three algorithms in the case of different numbers of IoT devices. The OPT-VCGRA mechanism has the highest execution time, the MDTRAP mechanism has the second highest execution time, and the first fit algorithm has the lowest execution time. As the number of IoT devices increases, the execution time of the OPT-VCGRA mechanism increases rapidly, and when the number of IoT devices exceeds 1000, the OPT-VCGRA mechanism cannot produce a solution. Therefore, the OPT-VCGRA mechanism cannot be used to solve the real-world base station resource allocation problem for large numbers of IoT devices, which is a disadvantage of the OPT-VCGRA mechanism. The execution time of the MDTRAP mechanism is much smaller than that of the OPT-VCGRA mechanism, and the social welfare obtained by both mechanisms is similar, which is an advantage of the MDTRAP mechanism. Although the first fit algorithm has the shortest execution time, the social welfare obtained by the algorithm differs significantly from that of the other two mechanisms, and from a systematic perspective, applying the first adaptation algorithm to solve the resource allocation results is the worst choice.

Figure 6 represents the total amounts paid by the VSP to the IoT devices in both mechanisms under different numbers of IoT devices. The MDTRAP mechanism has a much lower payment than does the OPT-VCGRA mechanism. Similar to the experimental results from the above experiments, as the number of winners increases, the difference in the amount of VSP payments in the two mechanisms increases. The difference is not eliminated as the number of channels and the number of IoT devices change.

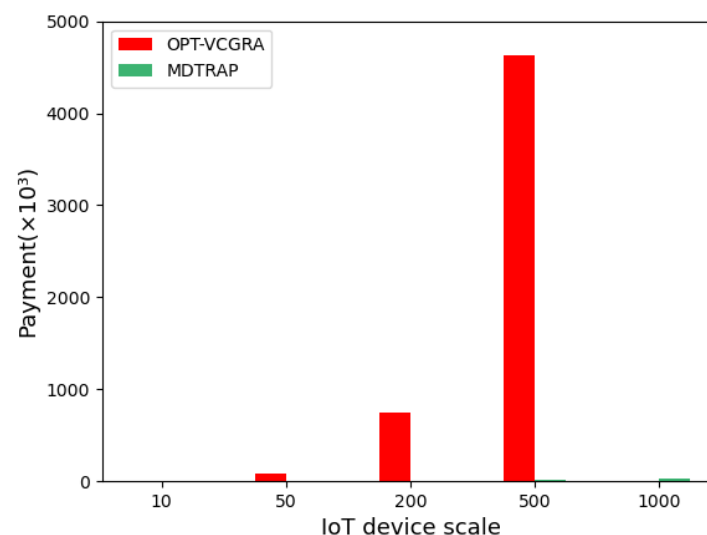


Figure 6. The total amount paid by the VSP to IoT devices under different numbers of IoT devices.

5.4. The Impact of the Number of UAVs on Allocation

In this experiment, we verified the impact of the number of UAV-BSs on allocation. The number of IoT devices $\mathcal{N} = 100$ and the number of UAV-BSs \mathcal{M} is 2, 5, 10 and 15. The number of channel resources provided by each UAV-BS is 50. Meanwhile, we assume that the unit of data transmitted by a device is Mb. The channel resources provided by UAV base stations do not satisfy the demands of all IoT devices, so they can be used to simulate the real-world situation where base stations have limited resources. This experiment compares different aspects of the OPT-VCGRA mechanism, the MDTRAP mechanism and the first fit algorithm in the case of different numbers of UAV base stations.

Figure 7a represents the social welfare of the three algorithms in the case of different numbers of UAV-BSs. The OPT-VCGRA mechanism has the largest social welfare, the MDTRAP mechanism has the second largest social welfare, and the first fit algorithm has the smallest social welfare. Similar to the above experimental results. The OPT-VCGRA mechanism solves the allocation problem from the perspective of the global optimization of social welfare, and the MDTRAP mechanism solves the allocation problem from the perspective of the local optimization of social welfare. The first fit algorithm

does not consider social welfare but only the order in which IoT devices request resources. Therefore, the results of this experiment are similar to the results of the two experiments above. However, the social welfare obtained by the MDTRAP mechanism is similar to the optimal result of the OPT-VCGRA mechanism, so the MDTRAP mechanism is the suboptimal choice when the OPT-VCGRA mechanism cannot solve for the optimal result.

Figure 7b represents the number of winners for the three algorithms under different numbers of UAV-BSs.

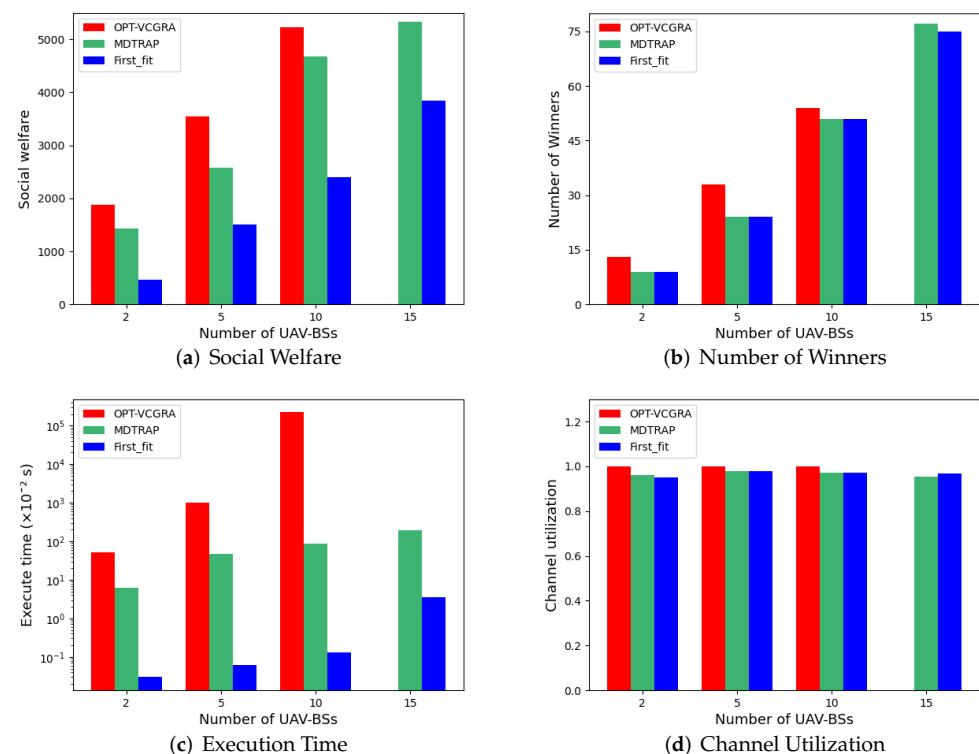


Figure 7. Social welfare, number of winners, execution time and channel utilization under different numbers of UAV-BSs.

The number of winners solved by the three algorithms is similar. The size of the data transmitted by IoT devices does not differ substantially, so the number of requests from devices for channel resources is similar. With the same channel resources, all three algorithms allocate as many channel resources to IoT devices as possible, so the three algorithms have a similar number of winners, which is also similar to the results of the two experiments above. Figure 7d represents the channel utilization of the three algorithms under different numbers of UAV-BSs. Since the number of winners of the three algorithms is similar and the channel resource requirements of IoT devices are similar, the utilization of channel resources by the three algorithms is similar and close to 1. The results of this experiment are also similar to those of the two experiments above.

Figure 7c represents the execution times of the three algorithms under different numbers of UAV-BSs. The execution time of the OPT-VCGRA mechanism is much longer than that of the other two algorithms. We take the logarithm of the execution time for the three algorithms and use the obtained order of magnitude as the vertical coordinate. From the figure, we can see that the execution time of the OPT-VCGRA mechanism is orders of magnitude higher than that of the MDTRAP mechanism. As the number of UAV base stations increases, the execution time of the OPT-VCGRA mechanism increases rapidly. When the number of UAV base stations is 15, the OPT-VCGRA mechanism cannot obtain the optimal result, while the MDTRAP mechanism can obtain the result in a short time.

Figure 8 represents the total amount paid by the VSP in both mechanisms under different numbers of UAV base stations. Similar to the results of the two experiments above,

the payment amount of VSP in the OPT-VCGR mechanism is much larger than that in the MDTRAP mechanism. From the perspective of the VSP, the MDTRAP mechanism is beneficial.

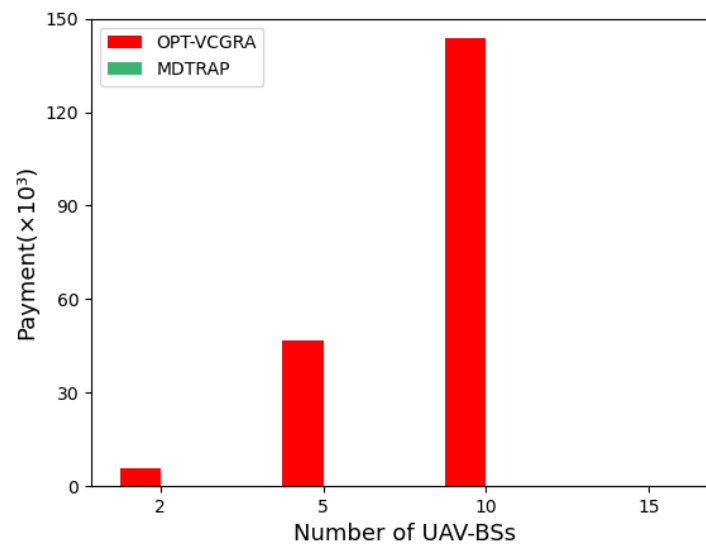


Figure 8. The total amount paid by the VSP to IoT devices under different numbers of UAV-BSs.

From the results of the three experiments, we can see that the social welfare, number of winners, and channel utilization obtained by the MDPRAP mechanism are close to the optimal results calculated by the OPT-VCGR mechanism, but the execution time of the MDTRAP mechanism is much shorter than that of the OPT-VCGR mechanism. Moreover, the payment amount of the VSP in the MDTRAP mechanism is also much smaller than that of the OPT-VCGR mechanism. In addition, the execution time of the OPT-VCGR mechanism increases rapidly when the number of IoT devices or UAV-BSs increases. When the number of IoT devices or UAV-BSs increases to a certain value, the OPT-VCGR mechanism cannot solve for the optimal result. However, the MDTRAP mechanism can solve for the allocation result in a short time, and according to our experiments, the result approximates the optimal result of the OPT-VCGR mechanism. Therefore, we can conclude that the MDTRAP mechanism can be used to solve the problem of allocating resources for large-scale IoT devices by a larger number of UAV-BSs in the real world.

5.5. Truthfulness Verification of MDTRAP

This experiment verifies the truthfulness of the MDTRAP mechanism from two perspectives: (1) the bid of the winner is changed to observe its utility changes and (2) the bid of the loser is changed to observe its utility changes. The experimental results are shown in Figure 9.

Figure 9a represents the change in utility when the bid of winner 1 is changed. The truthful bids of IoT device 1, which transmits data through base stations 1 and 2, are 46.1 and 69.5, respectively, and according to the allocation algorithm in the MDTRAP mechanism, IoT device 1 is selected by base station 1 for resource allocation. Moreover, when IoT device 1 wins, the amount paid by the VSP to IoT device 1 is 90.92, and its utility is 44.82. By continuously changing the bid of device 1 (for different base stations), it can be found that as long as the bid is lower than 87.9 (since we have limited resources to satisfy all devices, this limit may be lower than the amount paid by the VSP), the device can still win, and its utility remains the same.

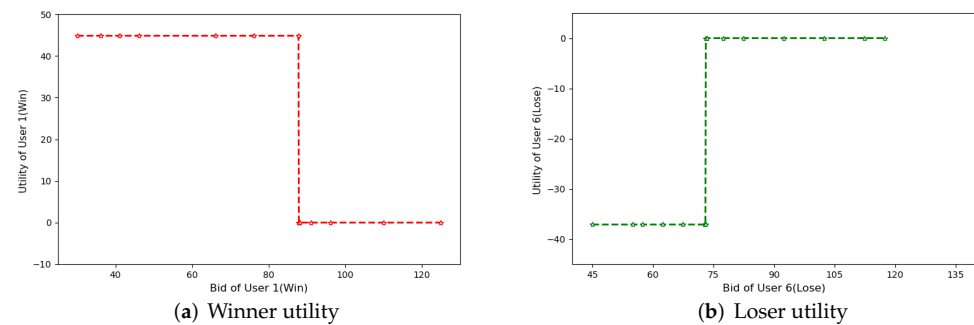


Figure 9. Truthfulness verification.

This is because the payment algorithm in the MDTRAP mechanism ensures that changing the bid of an IoT device that wins does not change the key value, so changing the bid when the IoT device wins does not affect the payment amount and the utility remains the same. When the bid is higher than this limit, the IoT device becomes a loser, and the utility becomes 0.

Figure 9b represents the change in utility when changing the bid of loser 6. The truthful bids of IoT device 6 that transmits data through base stations 1 and 2 are 115.6 and 112.4, respectively. Since IoT device 6 is the loser, the payment amount that the VSP gives to IoT device 6 is 0, and the utility is 0. When the bid for device 6 is higher than 73.1, it cannot be the winner, and its utility remains 0. However, when the bid of device 6 is lower than 73.1, device 6 wins in the allocation phase, and the amount paid by the VSP to IoT device 6 is 75.28, but the utility of IoT device 6 is $75.28 - 112.4 = -37.12$. The two examples show that users cannot change their bids to obtain greater utility and verify the truthfulness of the MDTRAP mechanism.

6. Conclusions

This paper investigates the problem of allocating wireless channel resources for IoT devices by multiple UAV base stations sent by the VSP when constructing a metaverse using digital twins. We design a reverse auction mechanism to maximize social welfare and solve the problem of IoT devices competing for base station resources. Specifically, by solving the problem of IoT devices competing for the channel resources of multiple base stations sent by the VSP and the payment scheme based on the VCG mechanism, we design an optimal VCG reverse auction mechanism to achieve the optimal allocation that maximizes social welfare and calculate the payment price. In addition, based on the price per unit data value of IoT devices, we design a metaverse digital twin resource allocation and pricing mechanism to solve the results of resource allocation by a large number of base stations to large-scale IoT devices when building metaverses in the real world and calculate the payment price. We also prove that both auction mechanisms have the properties of incentive compatibility and individual rationality. In addition, we designed several experiments to assess the impacts of the number of channels, the number of IoT devices, and the number of UAV-BSs on allocation and to verify the truthfulness of the MDTRAP mechanism. Each experiment compares the MDTRAP mechanism, the OPT-VCGRA mechanism, and the first adaptation algorithm in terms of social welfare, the number of winners, and total payments, and verifies that the results of the MDTRAP mechanism approximate the optimal results of the OPT-VCGRA mechanism and that the execution time of the MDTRAP mechanism is much smaller than that of the OPT-VCGRA mechanism. Meanwhile, the payment amount of the VSP in the MDTRAP mechanism is much smaller than that of the OPT-VCGRA mechanism, so the MDTRAP mechanism is more beneficial to the VSP. Therefore, the MDTRAP mechanism can be used to solve the resource allocation problem for a large number of base stations and a large scale of IoT devices when building a metaverse in the real world and to calculate the price paid. Meanwhile, there are still many important issues worth investigating in the field of building a metaverse using digital twin technology. The

system we propose is an abstract consideration of real-world scenarios. In the real situation, the system may encounter IoT devices that use multiple base stations to transmit data to the VSP, or the resources requested by IoT devices may not be limited to channel resources but may include resources such as storage space, or the system may experience data loss and other communication problems when transmitting data. Our future research will focus on solving these problems. Furthermore, we will focus on applying reinforcement learning to the multibase station resource allocation problem to find a more rational and smarter method of resource allocation.

Author Contributions: Conceptualization, J.Z. and W.L.; methodology, J.Z.; software, M.Z.; validation, J.Z. and M.Z.; resources, J.Z.; writing—original draft preparation, M.Z.; writing—review and editing, J.Z. and W.L.; supervision, J.Z. and W.L.; funding acquisition, J.Z. All authors have read and agreed to the published version of the manuscript.

Funding: This work is supported in part by the National Natural Science Foundation of China (Nos. 62062065, 12071417, 61962061), a project of the Natural Science Foundation of Yunnan Province of China (2018ZF017), the Education Foundation of Yunnan Province of China (2022J002) and the Program for Excellent Young Talents, Yunnan, China, a major projects of Yunnan Province of China (No. 202202AD080007), the 14th Postgraduate Research Innovation Fund Project of Yunnan University (No. KC-22221592).

Data Availability Statement: The reader can find the original data in the paper in <https://competition.huaweicloud.com/codecraft2022> accessed on 1 October 2022. The reader can find the data required and generated for the experiments in the paper in <https://github.com/zongmingyi/MDTRAP> accessed on 1 October 2022.

Conflicts of Interest: The authors declare no conflict of interest.

References

- Jeong, H.; Yi, Y.; Kim, D. An Innovative E-Commerce Platform Incorporating Metaverse to Live Commerce. *Int. J. Innov. Comput. Inf. Control* **2022**, *18*, 221–229. [CrossRef]
- Papyshev, G.; Yarime, M. Exploring city digital twins as policy tools: A task-based approach to generating synthetic data on urban mobility. *Data Policy* **2021**, *3*, e16. [CrossRef]
- Minerva, R.; Lee, G.M.; Crespi, N. Digital Twin in the IoT Context: A Survey on Technical Features, Scenarios, and Architectural Models. *Proc. IEEE* **2020**, *108*, 1785–1824. [CrossRef]
- Chen, M.; Saad, W.; Yin, C. Virtual reality over wireless networks: Quality-of-service model and learning-based resource management. *IEEE Trans. Commun.* **2018**, *66*, 5621–5635. [CrossRef]
- Chang, L.; Zhang, Z.; Li, P.; Xi, S.; Guo, W.; Shen, Y.; Xiong, Z.; Kang, J.; Niyato, D.; Qiao, X.; et al. 6G-enabled Edge AI for Metaverse: Challenges, Methods, and Future Research Directions. *arXiv* **2022**, arXiv:2204.06192.
- Hong, J.S.; Han, D.H.; Kim, Y.I.; Bae, S.J.; Kim, S.M.; Renshaw, P. English language education on-line game and brain connectivity. *ReCALL* **2017**, *29*, 3–21. [CrossRef]
- Zhang, J.; Lou, W.; Sun, H.; Su, Q.; Li, W. Truthful auction mechanisms for resource allocation in the Internet of Vehicles with public blockchain networks. *Future Gener. Comput. Syst.* **2022**, *132*, 11–24. [CrossRef]
- Ruohomäki, T.; Airaksinen, E.; Huuska, P.; Kesäniemi, O.; Martikka, M.; Suomisto, J. Smart City Platform Enabling Digital Twin. In Proceedings of the 2018 International Conference on Intelligent Systems (IS), Funchal, Portugal, 25–27 September 2018; pp. 155–161. [CrossRef]
- Ismail, L.; Niyato, D.; Sun, S.; In Kim, D.; Erol-Kantarci, M.; Miao, C. Semantic Information Market For The Metaverse: An Auction Based Approach. *arXiv* **2022**, arXiv:2204.04878.
- Yan, G.; Olariu, S.; Weigle, M.C.; Abuelela, M. SmartParking: A Secure and Intelligent Parking System Using NOTICE. In Proceedings of the 2008 11th International IEEE Conference on Intelligent Transportation Systems, Beijing, China, 12–15 October 2008; pp. 569–574. [CrossRef]
- Zhang, Y.; Zhang, J. Design and Optimization of Cluster-Based DSRC and C-V2X Hybrid Routing. *Appl. Sci.* **2022**, *12*, 6782. [CrossRef]
- Cai, Y.; Llorca, J.; Tulino, A.M.; Molisch, A.F. Compute- and Data-Intensive Networks: The Key to the Metaverse. In Proceedings of the 2022 1st International Conference on 6G Networking (6GNet), Paris, France, 6–8 July 2022; pp. 1–8. [CrossRef]
- Lv, Z.; Qiao, L.; Li, Y.; Yuan, Y.; Wang, F.Y. BlockNet: Beyond reliable spatial Digital Twins to Parallel Metaverse. *Patterns* **2022**, *3*, 100468. [CrossRef]
- Lin, Z.; Xiangli, P.; Li, Z.; Liang, F.; Li, A. Towards Metaverse Manufacturing: A Blockchain-based Trusted Collaborative Governance System. In Proceedings of the ICBCT'22: The 2022 4th International Conference on Blockchain Technology, Shanghai, China, 25–27 March 2022; pp. 171–177. [CrossRef]

15. Ng, W.C.; Yang Bryan Lim, W.; Ng, J.S.; Xiong, Z.; Niyato, D.; Miao, C. Unified Resource Allocation Framework for the Edge Intelligence-Enabled Metaverse. In Proceedings of the ICC 2022—IEEE International Conference on Communications, Seoul, Republic of Korea, 16–20 May 2022; pp. 5214–5219. [\[CrossRef\]](#)
16. Zhang, J.; Yang, X.; Xie, N.; Zhang, X.; Vasilakos, A.V.; Li, W. An online auction mechanism for time-varying multidimensional resource allocation in clouds. *Future Gener. Comput. Syst.* **2020**, *111*, 27–38. [\[CrossRef\]](#)
17. Chu, N.H.; Hoang, D.T.; Nguyen, D.N.; Phan, K.T.; Dutkiewicz, E. MetaSlicing: A Novel Resource Allocation Framework for Metaverse. *arXiv* **2022**, arXiv:2205.11087.
18. Zhang, J.; Chi, L.; Xie, N.; Yang, X.; Zhang, X.; Li, W. Strategy-proof mechanism for online resource allocation in cloud and edge collaboration. *Computing* **2022**, *104*, 383–412. [\[CrossRef\]](#)
19. Chen, Y.L.; Huang, S.Y.; Chang, Y.C.; Chao, H.C. Resource Allocation based on Genetic Algorithm for Cloud Computing. In Proceedings of the 2021 30th Wireless and Optical Communications Conference (WOCC), Taipei, Taiwan, 7–8 October 2021; pp. 211–212. [\[CrossRef\]](#)
20. Nagpure, M.B.; Dahiwal, P.; Marbate, P. An efficient dynamic resource allocation strategy for VM environment in cloud. In Proceedings of the 2015 International Conference on Pervasive Computing (ICPC), Pune, India, 8–10 January 2015; pp. 1–5. [\[CrossRef\]](#)
21. Alam, A.B.M.B.; Zulkernine, M.; Haque, A. A Reliability-Based Resource Allocation Approach for Cloud Computing. In Proceedings of the 2017 IEEE 7th International Symposium on Cloud and Service Computing (SC2), Kanazawa, Japan, 22–25 November 2017; pp. 249–252. [\[CrossRef\]](#)
22. Han, Y.; Niyato, D.; Leung, C.; Miao, C.; In Kim, D. A Dynamic Resource Allocation Framework for Synchronizing Metaverse with IoT Service and Data. *arXiv* **2021**, arXiv:2111.00431.
23. Chengoden, R.; Victor, N.; Huynh-The, T.; Yenduri, G.; Jhaveri, R.H.; Alazab, M.; Bhattacharya, S.; Hegde, P.; Maddikunta, P.K.R.; Gadekallu, T.R. Metaverse for Healthcare: A Survey on Potential Applications, Challenges and Future Directions. *arXiv* **2022**, arXiv:2209.04160. <https://doi.org/10.48550/ARXIV.2209.04160>.
24. Zhong, E.; Li, P.; Zhang, T.; Huang, W.; Liu, Q. Mobile Data Offloading in the Vehicular Networks: A Truthful Incentive Mechanism. In Proceedings of the 2019 IEEE 21st International Conference on High Performance Computing and Communications; IEEE 17th International Conference on Smart City; IEEE 5th International Conference on Data Science and Systems (HPCC/SmartCity/DSS), Zhangjiajie, China, 10–12 August 2019; pp. 2206–2211. [\[CrossRef\]](#)
25. Zhang, J.; Xie, N.; Zhang, X.; Li, W. Strategy-Proof Mechanism for Online Time-Varying Resource Allocation with Restart. *J. Grid Comput.* **2021**, *19*, 25. [\[CrossRef\]](#)
26. Xu, J. A Cloud Computing Resource Allocation Model Based on Combinatorial Double Auction. In Proceedings of the 2016 3rd International Conference on Information Science and Control Engineering (ICISCE), Beijing, China, 8–10 July 2016; pp. 5–8. [\[CrossRef\]](#)
27. Chichin, S.; Bao Vo, Q.; Kowalczyk, R. Adaptive Market Mechanism for Efficient Cloud Services Trading. In Proceedings of the 2014 IEEE 7th International Conference on Cloud Computing, Anchorage, AK, USA, 2–27 July 2014; pp. 705–712. [\[CrossRef\]](#)
28. Zhang, J.; Xie, N.; Yang, X.; Zhang, X.; Li, W. Strategy-Proof Mechanism for Time-Varying Batch Virtual Machine Allocation in Clouds. *Clust. Comput.* **2021**, *24*, 3709–3724. [\[CrossRef\]](#)
29. Zaman, S.; Grosu, D. An Online Mechanism for Dynamic VM Provisioning and Allocation in Clouds. In Proceedings of the 2012 IEEE Fifth International Conference on Cloud Computing, Honolulu, HI, USA, 24–29 June 2012; pp. 253–260. [\[CrossRef\]](#)
30. Thi Le, T.H.; Tran, N.H.; Tun, Y.K.; Nguyen, M.N.H.; Pandey, S.R.; Han, Z.; Hong, C.S. An Incentive Mechanism for Federated Learning in Wireless Cellular Networks: An Auction Approach. *IEEE Trans. Wirel. Commun.* **2021**, *20*, 4874–4887. [\[CrossRef\]](#)
31. Jiao, Y.; Wang, P.; Niyato, D.; Lin, B.; Kim, D.I. Toward an Automated Auction Framework for Wireless Federated Learning Services Market. *IEEE Trans. Mob. Comput.* **2021**, *20*, 3034–3048. [\[CrossRef\]](#)
32. Lee, H.; Park, S.; Kim, J.; Kim, J. Auction-based Deep Learning Computation Offloading for Truthful Edge Computing: A Myerson Auction Approach. In Proceedings of the 2021 International Conference on Information Networking (ICOIN), Jeju Island, Republic of Korea, 13–16 January 2021; pp. 457–459. [\[CrossRef\]](#)
33. Zhu, K.; Xu, Y.; Jun, Q.; Niyato, D. Revenue-Optimal Auction For Resource Allocation in Wireless Virtualization: A Deep Learning Approach. *IEEE Trans. Mob. Comput.* **2022**, *21*, 1374–1387. [\[CrossRef\]](#)
34. Available online: <https://www.cambricon.com> (1 October 2022).
35. Yeo, H. Autonomous Driving Technology through Image Classification and Object Recognition Based on CNN. In Proceedings of the 2020 4th International Conference on Vision, Image and Signal Processing, Bangkok, Thailand, 9–12 December 2020; Association for Computing Machinery: New York, NY, USA, 2020; ICVIS 2020. [\[CrossRef\]](#)
36. Available online: <https://competition.huaweicloud.com/codecraft2022> (1 July 2022).